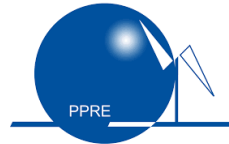




Carl von Ossietzky Universität Oldenburg

Institute of Physics

Postgraduate Programme Renewable Energy



Master's Thesis

Title:

*Technology Pathways for Transforming High Temperature to Low  
Temperature District Heating Systems in the ENaQ Project*

Presented by: *Pedro Durán Hermosilla*

First examiner: *Dr. Herena Torio*

Second examiner: *Prof. Dr. Carsten Agert*

Place, Date: *Oldenburg, 21.08.2020*

## Abstract

In Germany there are 1454 district heating systems. Most of them are fossil fuel based and with high temperature levels. The ENaQ project located in Oldenburg proposes a high temperature district heating system (HTDH). This master thesis takes this project as a reference and studies the feasibility of transforming its high temperature to a low temperature district heating system (LTDH). The main objective of this study is to technically understand what is needed in order to perform the system transformation. The results found here are presented as guidelines that can be applied at other systems that aim to reduce its operating temperature.

Four steps were carried out to perform this master thesis. The first was to develop and validate a dynamic LTDH model as a reference scenario with the Carnot Toolbox from Simulink in the Matlab software. Then the ENaQ HTDH (initial scenario) was modeled. The third step was to take the data and constraints used in ENaQ HTDH and merge them with the validated LTDH model to perform the high to low temperature system transformation. At this point both models are compared by 5 indicators to observe the difference between them. Since the LTDH model makes use of more space, specially because of the implementation of decentralized storage tanks and a seasonal storage, the last step was to perform a sensitivity analysis of ENaQ LTDH to see how the system performance changes in case there are economic or space constraints that would not allow the transformation 100% to happen.

Results show that it is technically possible to perform the district heating system transformation until the very LTDH where the share of renewable energy sources increases from 0.3% to 84%, transport losses and greenhouse gas emissions are reduced from 8.3% to 3.4% and from 135 to 57 tCO<sub>2</sub>eq respectively. The two key points that allow this transformation to happen are the placement of a heat pump at the outlet of each building, which makes it possible to reduce the return temperature of the district network and consequently the supply temperature, and the implementation of decentralized heat sources on each building that reduces the transported energy through the network. Regarding the sensitivity analysis, the developed guidelines propose that in case the seasonal storage is limited, the transformation is worth doing until it reaches a size of 60% of the proposed nominal value (6198 [m<sup>3</sup>]). In case the solar collector area is limited, the transformation is still worth it until it reaches 80% of the proposed nominal value (915 [m<sup>2</sup>] in total). Finally, in case there is space for only one decentralized storage, the transformation is still worth doing, however it is necessary to study if the transformation is hydraulically feasible since there are constant changes in the mass flow direction in the district network.

*A mis abuelas Edith y María*

# Declaration

I state and declare that this master thesis was prepared by me and that no means or sources have been used, except those, which I cited and listed in the Bibliography section. The master thesis is in compliance with the rules of good practice in scientific research of Carl von Ossietzky Universität Oldenburg

# Acknowledgments

This master thesis marks the closing of a two years cycle. Much more than the PPRE cycle it marks a transition cycle in my life which brought me, as usual, good and bad experiences. Fortunately, the good experiences overcome the bad ones and I am very happy to have made the decision to come to Germany. There is a lot of people to thank for me writing this now.

In the first place I would like to thank my first family, to my sister Camila and my mother Ada that despite the 12.241 km distance are my pillar and they have always been there for supporting me and sharing good and bad moments.

In the second place I would like to thank my second family, my friends in Oldenburg, for those countless moments of conversations, laughs, bike rides, games and drinks, to Adrian, Fabio, Daniela, Alejandro but specially to Mafe in whom I found understanding, complicity, brotherhood and a home. Obviously I want to thank Kira who accompanied me in this process for a long time which means a lot to me, a part of this work is also hers.

This master thesis would not have been possible without the support of the Deutsches Zentrum für Luft- und Raumfahrt, specifically the Institut für Vernetzte Energiesysteme, which opened its doors to me more than a year ago allowing me to learn many things from seeing how a research center works to giving me the opportunity to meet highly specialized people in different disciplines. Under this frame I want to thank my supervisors who helped me get this thesis done: Dr. Herena Torio for those endless discussions about technical aspects but more important for those discussions about life itself and her unconditional support and to Dr. Peter Klement for always being available for any questions, open to any proposal and encouraging new ideas. Spacial thanks to Prof. Dr. Carsten Agert for agreeing to be my examiner.

Last but not least, I would like to thanks to the Technische Universität München, scepiclly to Thomas Auer, Isabell Nemeth and Karl Martin Heißler, for providing me, without any problem, the necessary data to develop my models.

# Contents

<b>1</b>	<b>Introduction</b>	<b>1</b>
1.1	Motivation . . . . .	1
1.2	Problem description . . . . .	2
1.2.1	Energetic Neighbourhood Quarter (ENaQ) project . . . . .	5
1.3	Thesis structure . . . . .	6
<b>2</b>	<b>Theory</b>	<b>7</b>
2.1	High temperature district heating systems . . . . .	7
2.2	Low temperature district heating systems . . . . .	8
2.3	Challenges for reducing a district heating system temperature . . . . .	9
2.4	The Carnot Toolbox . . . . .	10
<b>3</b>	<b>Methodology</b>	<b>12</b>
3.1	Develop and validation of a dynamic LTDH model as reference scenario	13
3.1.1	Reference case: TUM study . . . . .	14
3.1.2	Single building model in the Carnot Toolbox . . . . .	17
3.1.3	Scaling up method to represent the whole district heating system in the Carnot Toolbox . . . . .	19
3.1.4	Functional validation of the Carnot Toolbox model . . . . .	23
3.2	Model ENaQ starting scenario (HTDH) . . . . .	32
3.3	Model ENaQ retrofitted scenario (LTDH) . . . . .	34
3.4	Development of key performance indicators to compare different scenarios . . . . .	35
3.5	Sensitivity analysis of ENaQ retrofitted scenario . . . . .	36
3.5.1	ENaQ retrofitted with different solar collector area and different seasonal storage volume . . . . .	37
3.5.2	ENaQ retrofitted with only one decentralized storage . . . . .	37
<b>4</b>	<b>Results and Discussion</b>	<b>39</b>

4.1	Comparison between ENaQ starting (HTDH) and ENaQ retrofitted (LTDH) scenario . . . . .	39
4.2	Sensitivity analysis of ENaQ retrofitted (LTDH) scenario . . . . .	47
4.2.1	ENaQ retrofitted with different solar collector area and different seasonal storage volume . . . . .	47
4.2.2	ENaQ retrofitted with only one decentralized storage tank . . .	57
<b>5</b>	<b>Conclusion and Future Work</b>	<b>62</b>
5.1	Conclusion . . . . .	62
5.2	Future work . . . . .	64
	<b>Bibliography</b>	<b>66</b>
<b>A</b>	<b>Heat Pump data used in the Model</b>	<b>69</b>
<b>B</b>	<b>Images of LTDH model developed in the Carnot Toolbox</b>	<b>71</b>

# List of Figures

1.1	Complete picture for implementing LTDH systems and the part covered in this master thesis (marked green) . . . . .	3
3.1	General overview of the methodology . . . . .	12
3.2	Software coupling of the TUM model (Figure translated from [28, p. 15]) . . . . .	14
3.3	Building technology system of the reference scenario (Figure translated from [28, p. 19]) . . . . .	15
3.4	Pipe structure of the reference scenario (Figure translated from TUM [28, p. 28]) . . . . .	17
3.5	Scheme of the 4 pipes network modeled in the Carnot Toolbox . . . .	20
3.6	Results comparison between TUM (Figure translated from [28, p. 63]) and Carnot Toolbox model: General Overview . . . . .	24
3.7	Results comparison between TUM (Figure translated from [28, p. 63]) and Carnot Toolbox model: Monthly shares of energy by source and demand covered . . . . .	25
3.8	Results comparison between TUM (Figure translated from [28, p. 64]) and Carnot Toolbox model: Monthly energy balance between the district network and the seasonal storage . . . . .	26
3.9	Results comparison between TUM (Figure translated from [28, p. 64]) and Carnot Toolbox model: Network temperature . . . . .	27
3.10	Results comparison between TUM (Figure translated from [28, p. 65]) and Carnot Toolbox model: Monthly losses in the district network	29
3.11	Results comparison between TUM and Carnot Toolbox model: Sankey diagram . . . . .	30
3.12	ENaQ district heating system (Figure obtained from GSG company)	32
3.13	Scheme of ENaQ HTDH . . . . .	34
3.14	ENaQ building technology reconfiguration for operating with one decentralized storage tank (Figure modified from [28] p.19) . . . . .	38



4.1	Hourly and daily network temperature at ENaQ starting scenario for one year . . . . .	40
4.2	Hourly and daily network temperature at ENaQ retrofitting scenario for one year . . . . .	41
4.3	Monthly transported energy through the district network for ENaQ HT and LT . . . . .	42
4.4	Monthly transported energy through the network for ENaQ HT and LT . . . . .	43
4.5	Share of renewable energy used for different sizes of solar collector field and seasonal storage tank . . . . .	48
4.6	Share of electricity used for different sizes of solar collector field and seasonal storage tank . . . . .	50
4.7	Share of energy taken from network for different sizes of solar collector field and seasonal storage tank . . . . .	51
4.8	Transport losses for different sizes of solar collector field and seasonal storage tank . . . . .	53
4.9	Greenhouse gas emissions for different sizes of solar collector field and seasonal storage tank . . . . .	54
4.10	Flow direction signal in the district network for the one decentralized storage tank system . . . . .	60
4.11	Flow direction signal in the district network for the two decentralized storage tank system . . . . .	61
A.1	Heat pump data used in the reference model provided by the Technical University of Munich . . . . .	69
A.2	Heat pump curves in the form the Carnot Toolbox uses it. Curves derived from the data provided by the TUM . . . . .	70
B.1	Solar collector field modeled in the Carnot Toolbox . . . . .	72
B.2	On-demand storage with SH and DHW demands modeled in the Carnot Toolbox . . . . .	72
B.3	Buffer storage tank, heat pump and connection with the network modeled in the Carnot Toolbox . . . . .	73
B.4	District network with the seasonal storage modeled in the Carnot Toolbox . . . . .	73

# List of Tables

1.1	Goals for GHG reduction and share of renewable sources for Germany	1
3.1	Results comparison between TUM and Carnot Toolbox model: general overview	24
3.2	Share of heat sources for TUM and Carnot Toolbox	31
3.3	Share of heat sinks for TUM and Carnot Toolbox	31
3.4	Area, SH and DHW specific demand for each building in ENaQ project	33
3.5	Solar collector area, buffer and on-demand storage sizes for building 3b	35
4.1	KPI to compare ENaQ starting and ENaQ retrofitted scenario	43
4.2	KPI modified to compare ENaQ retrofitted and LTDH reference scenario	46
4.3	KPI comparison between ENaQ retrofitted with one and two decentralized storage tanks	58

# List of Abbreviations

HTDH	High temperature district heating
LTDH	Low temperature district heating
RE	Renewable energy
NRE	Non renewable energy
GHG	Greenhouse gas
KPI	Key performance indicator
TUM	Technical University of Munich
SH	Space heating
DHW	Domestic hot water
CHP	Combined heat and power
PVT	Photovoltaic thermal collector
HP	Heat pump
HE	Heat exchanger
COP	Coefficient of performance
OdS	On-demand storage
BS	Buffer storage
$ST_{dir}$	Solar thermal direct
EL	Electricity
Q	Heat
$W_{el}$	Electricity used (Sankey diagram)

# Chapter 1

## Introduction

### 1.1 Motivation

The “Climate Action Plan 2050” [1] from the German Federal Government is aiming for a reduction of greenhouse gases (GHG) between 85% and 95% by 2050 compared to 1990 levels in order to keep the increase of the global average temperature below 2°C [2]. An intermediate step for this is the 2030 goal: a reduction of GHG emission of 55% compared to 1990 levels. To achieve these reductions, the share of energy coming from renewable sources needs to increase. Table 1.1 shows an overview of the German goals in terms of GHG reduction and share of renewable sources in the energy consumption [3, p. 9].

	<b>2020</b>	<b>2030</b>	<b>2050</b>
<b>GHG reduction compared to 1990 levels</b>	40%	55%	80 to 95%
<b>Share of RE sources in the total final energy consumption</b>	18%	65%	80%

Table 1.1: Goals for GHG reduction and share of renewable sources for Germany

The plan proposes different reduction goals for the different sectors: power, heat and mobility not only by increasing the share of energy coming from renewable sources but also by improving each sector efficiency which generates a reduction on the final energy consumption.

Narrowing the scope to the heating sector, in 2050 Germany aims to reduce their heat demand by 80% compared to 2008 levels [3, p. 9]. As said before, two strategies in parallel must be carried out: the increase of renewable sources and the improvement

in the sector efficiency. Low temperature district heating systems (LTDH), so-called Low-Ex networks [4] address these two key points in the building sector: from one side by including renewable sources on the district heating systems and from the other side by reducing the system losses which improves the efficiency of the supply system. Moreover LTDH aim at balancing the quality level at which energy demands are supplied, maximizing the use of low temperature sources for providing low temperature demands and minimizing the temperature levels in the district network. Such innovative district heating systems concepts are identified as a key milestone in the “Climate Action Plan 2050” of the German government. Low temperature district heating systems rely on efficient technologies for sector coupling such as heat pumps or PVT, technologies for converting radiation into heat such as solar collectors and technologies to save the surplus of energy produced during summer and use it in winter for example seasonal storage tanks.

Going back to the emissions targets from the “Climate Action Plan 2050” and specifically into the building sector a reduction of 67% of the CO<sub>2</sub> emissions shall be achieved by 2030. This reduction shall be accomplished by three main measures [5]:

1. Retrofitting the building stock and reducing its energy demands.
2. Implementing renewable energy sources for heat production.
3. Using renewable electricity for supplying heat demands.

Heat demands for space heating (SH) and domestic hot water (DHW) in the built environment amount to 469 [TWh/a] and represent 32% of the total final energy demands in Germany [3, p. 3]. But whereas the renewable energy share in the electricity sector amounts to 42.1% of the consumption, this share represents merely 14.5% and 5.6% in the heat and mobility sectors, respectively [6][7]. Therefore power-to-heat strategies are a promising field for implementing sector coupling solutions [8].

## 1.2 Problem description

Figure 1.1 describes the whole range where low temperature district heating systems can be implemented. LTDH can be implemented as as new system (right column) or by transforming (retrofitting) a high temperature into a low temperature one (3<sup>rd</sup> column). In a new system, the network design is very flexible since the system will be constructed to be used as a low temperature one. There is also a lot of

technological flexibility because of the same reason: there is the possibility of incorporate solar collectors, seasonal storage tanks or heat pumps among others. On the other hand in a retrofitted district heating system, there is already a system with its district network, which was built for operating at high temperatures. Therefore there is a constrained network design that needs to be taken into account for the implementation of a LTDH. Since the system will be retrofitted there is also space for incorporating new technologies and therefore a flexible technology design.

		Decreasing network temperature →		
Decreasing energy demands ↓		Existing DH System (HT)	Retrofitted DH System (HT → LT)	New DH System (LT)
	<b>Old buildings</b> Low efficiency SH demand about 200 kWh/m <sup>2</sup> a	Network design <b>Constrained</b>  Technology design <b>Constrained</b> (gas/oil boiler)	Network design <b>Constrained</b>  Technology design <b>Flexible</b> (stretch technology solutions to supply higher demands with low temperature)	Network design <b>Flexible</b>  Technology design <b>Flexible</b> (stretch technology solutions to supply higher demands with low temperature)
	<b>Retrofitted buildings</b> Medium efficiency SH demand between 75 and 150 kWh/m <sup>2</sup> a	Network design <b>Constrained</b>  Technology design <b>Constrained</b> (gas/oil boiler)	Network design <b>Constrained</b>  Technology design <b>Flexible</b> (find technology solutions to supply high demands with low temperature)	Network design <b>Flexible</b>  Technology design <b>Flexible</b> (find technology solutions to supply high demands with low temperature)
	<b>New buildings</b> High efficiency SH demand about 50 kWh/m <sup>2</sup> a	<b>ENaQ starting scenario</b>  Network design <b>Constrained</b>  Technology design <b>Constrained</b> (CHP/ gas boiler)	<b>ENaQ retrofitted scenario</b>  Network design <b>Constrained</b>  Technology design <b>Flexible</b>	<b>ENaQ aiming scenario</b>  Network design <b>Flexible</b>  Technology design <b>Flexible</b> (decentralized collectors and heat pumps, centralized seasonal storage)

Figure 1.1: Complete picture for implementing LTDH systems and the part covered in this master thesis (marked green)

In Germany, there are 1454 district heating systems, which represent the 13.8% of the heat sector [9]. From all these systems, 83% of the heat comes from CHP [10]. The previous means that most of existing district heating systems in Germany are high temperature ones and fossil fuels based (CHP fuel comes from coal (31%), lignite (12%), gas (36%), renewables (13%) and others (8%) [11, p. 39]). Because of that, these district heating systems should be transformed to LTDH in order to achieve the proposed emissions reduction by 2050.

Another important point that needs to be considered on this problem is the length of the systems in Germany since the main costs of implementing a new district heating system are the digging and pipe installation throughout the entire district [12]. In Germany 86% of district heating systems are larger than 100 km [13, p. 6]. Cases like Munich or Mannheim with 800 km length each or Berlin with about 2000 km divided into 9 systems are good examples of large district networks and potential candidates to be used as LTDH with the advantage of avoiding the installation costs.

At the same time, if observing Figure 1.1, LTDH can be implemented in old (upper row), retrofitted (middle row) and new (lower row) buildings. In this new classification of buildings, implementing a LTDH in new buildings is easier since the required energy demand and temperature levels are lower for old buildings and therefore less challenging to supply. Nevertheless in Germany only 11% of the buildings were erected after the year 2000 [3, p. 57] which are under the EnEV<sup>1</sup> regulation that aims to a reduce heat demands on buildings. Therefore if the implementation of low temperature heat networks wants to be addressed in the whole building sector, then it is also necessary to figure out how they can be implemented in buildings with higher specific demands.

Having observed the problem in its entirety, this master thesis addresses the transformation of a high temperature district heating system into a low temperature one for new buildings. This is because the ENaQ project considers only new buildings as will be described in section 1.2.1. That means, this project covers the green square on Figure 1.1, where the starting point, called **ENaQ starting scenario** is a high temperature system in new buildings and from this point, the district heating system will be retrofitted to reduce its operating temperature until converting it to **ENaQ retrofitted scenario** always having as a reference the LTDH scenario called **ENaQ aiming scenario**. In other words, the technologies implemented on **ENaQ starting scenario** will move it to the right to get as close as possible to **ENaQ aiming scenario**. Whether **ENaQ retrofitted scenario** can finally reach **ENaQ aiming scenario** or ends in an middle point between starting and aiming scenario, is analysed in this master thesis.

In such a context the main question arises of what is necessary to do in a high temperature district heating system to transform it in a low temperature one. For helping to answer the previous question, the following sub questions were developed:

- What innovative LTDH concepts are available currently?

---

<sup>1</sup>Energieeinsparverordnung (In English: Energy saving regulation) [14]

- What would be a meaningful LTDH base case to have as reference?
- What kind of indicators are suitable to compare different district heating systems?
- How do the indicators mentioned above change when the HTDH to LTDH transformation occurs?
- Which technologies have the higher impact on lowering the temperature of a district heating system?
- How close can a HTDH be adapted to operate as a LTDH?

This master thesis aims at answering the above mentioned questions. It provides a basis for avoiding technology lock-ins which could be disadvantageous for the implementation of low temperature district heating systems, thus enhancing the potential for an effective use of such concepts in the built environment.

### **1.2.1 Energetic Neighbourhood Quarter (ENaQ) project**

The Energetic Neighbourhood Quarter (ENaQ) project<sup>2</sup> [15] develops novel concepts for a future oriented energy management of a local energy system. Testing the energy system under real conditions is also part of the project. As a sub-project leader for the “Networked Physical Infrastructure”, the DLR Institute of Networked Energy Systems is in charge of the conception and planning of the physical infrastructure. A concept for the energy supply of the Energetic Neighbourhood Quarter at the former military air base in Oldenburg is developed, implemented and evaluated. The aim of the sub-project is to have an holistic view of the energy supply in order to identify optimization potential early and to be able to use it. The focus is on the sector-coupling of electricity and heat as well as the integration of mobility for individual houses as well as for the entire district.

In the heating sector of the project it will be developed a CHP based district heating system, which means to have a high temperature, not renewable energy based and centralized system. Nevertheless the lifetime of the project EnAQ is about 10 years. After that it will be discussed among the partners of the project, how they want to proceed with it. In such a context the transformation of the district heating system from high to low temperature is a very attractive idea. The steps needed to do the mentioned transformation will be found on this master thesis but this is

---

<sup>2</sup>Original German name: Energetisches Nachbarschaftsquartier Fliegerhorst Oldenburg (FKZ: 03SBE111U)



not the final aim of this work. As said before ENaQ is the case study for finding technological pathways for transformation of district systems but the results found here can be applied at others high temperature systems which aims to reduce its operating temperature. This is the final aim of this study.

### 1.3 Thesis structure

This master thesis is organized as follows. In Chapter 2, proper theory about high and low temperature heat networks is described in order to understand what is necessary and what are the boundaries to transform a district heating system from high into a low temperature one. Chapter 3 shows in detail the methods and steps that were taken to perform this master thesis, from developing a LTDH model in the Carnot Toolbox platform from Simulink, going through model ENaQ district heating system as a high (**ENaQ starting scenario**) and then low temperature (**ENaQ retrofitted scenario**) districts to finally make a sensibility analysis of the last one in case there are economic or space constrains. In Chapter 4 the results of the mentioned models are shown and discussed together. Finally in Chapter 5 the conclusion and outlook of this study are presented.

# Chapter 2

## Theory

The concept of district heating system exists since the end of 19<sup>th</sup> century [16]. The first systems, called first generation, used steam as energy carrier, transported by concrete ducts, where the temperature level was above 100°C. After realizing the high risk of having pressurised steam across cities and also high share of losses due to high temperatures, the so called second generation came out around 1930. These systems used no more steam but pressurised hot water. Therefore temperature levels over 100°C were still a big source of losses. Nevertheless the primary energy consumption was reduced. The energy sources for these systems were coal, gas and oil.

Between 1970 and 1980, the third district heating system generation was introduced. These systems made use of hot water usually at temperature levels below 100°C with prefabricated components such isolated pipes or stainless steel heat exchangers in substations. With this, a reduction of heat losses was achieved. This system concept is nowadays widespread used in Europe, USA and China, among others. Beside coal, gas and oil, waste heat, industry surplus heat and occasionally biomass are the energy sources for these systems. In the last decade, the so called fourth district heating generation has been studied. This generation not only tries to reduce even more the district temperatures but also to include renewable energy sources. Then this generation not only seeks to improve the efficiency of the system but also to meet local and national GHG reduction targets [17].

### 2.1 High temperature district heating systems

After having reviewed the evolution of district heating systems, what in this master thesis is called high temperature district heating system (HTDH) corresponds to

the 3<sup>rd</sup> generation previously described. This means a HTDH is a system where hot water at temperature levels between 70°C and 100°C is transported. Although there is no strict concept of how the system structure is, there are some general rules that apply to most of cases:

- The district has a big central energy source, where the hot water is produced and transported to each building. The energy source can be a boiler or a CHP with a storage tank for dealing with peak loads. Both technologies can work with coal, oil, gas or waste [18].
- The district can also make use of industry heat surplus, which is feed into the network where the industry is located.
- Each building has a substation, where a heat exchanger is located allowing the heat transfer to the buildings. A small decentralized storage can be placed at the substation too [19].
- Supply temperatures are in the range between 70°C and 120°C [20] while return temperatures oscillate between 45°C and 65°C [21].
- Losses in the district heating system usually are in the range of 10% to 15% of the total generated energy [21] [17].

## 2.2 Low temperature district heating systems

Under the frame of this master thesis, what was described as 4<sup>th</sup> district heating system generation, is called low temperature district heating (LTDH). Since this system concept is relative new, there are no strict rules of how it should be. Nevertheless, and similarly to the HTDH, there are some guidelines that are suitable to describe them in most of cases:

- Both buildings and district heating network are treated as one integrated system, which generates synergies that can be optimized on a community scale. Moreover one of the future aims is to integrate district heating with the electricity sector as well as the transport sector [16]. Hence the use of digitization and smart systems are fundamental to couple all the edges of the system [17].
- The energy sources avoid the use of fossil fuels. Hence solar thermal, geothermal heat or heat pumps are the main technologies for providing heat.
- The concept of seasonal and decentralized storage is used to buffer the heat surplus produced in periods where there is no demand.

- Supply temperatures are in the range between 45°C and 55°C [17] while return temperatures are between 15°C 25°C [16].
- Losses in these systems usually are in the range of 5% to 10% of the total generated energy [17].

## 2.3 Challenges for reducing a district heating system temperature

Reducing the temperature of an existent district heating system is not a trivial problem. In the designing process of a district heating system, a certain supply and return temperature is set. From these design temperatures, different components of the system are calculated such as pipes isolation, size of heat exchangers, mass flow of the district network, pump sizes among others. Because of that, changing the system temperature means to change a parameter for which the system was designed, making it a big challenge. On an holistic view of the system, as this master thesis presents, there are two main challenges to overcome, in order to successfully achieve a temperature reduction.

The first point to address concerns the return temperature. It has been studied that the only way to reduce the district network temperature is by a reduction of the return temperature [22] [23]. Then a reduction of the return temperature leads to a reduction of the supply temperature and not vice versa. Therefore, the challenge here is to find technical solutions to reduce the return temperature of the system.

The second point concerns the water velocity inside the district network. Starting from the energy balance of the water flowing in the district network, Equation 2.1 [24, p. 290] shows that the energy transported by the water is equal to the multiplication of its specific heat, the mass flow and the difference between supply and return temperature.

$$\dot{Q}_{transported} = \dot{m}_w c_{pw} (T_{supply} - T_{return}) \quad (2.1)$$

Where:

- $\dot{Q}_{transported}$  = energy transported through the district network [W]
- $\dot{m}_w$  = mass flow of the water inside the district network [kg/s]
- $c_{pw}$  = specific heat of transport fluid, in this case water, 4.18 kJ/kgK

- $T_{supply}$  = water temperature going from the heat source to the buildings [°C]
- $T_{return}$  = water temperature going from the buildings to the heat source [°C]

When observing this equation, and knowing that the specific heat of water is a constant, there is a trade off between the mass flow and the  $\Delta T$  ( $T_{supply} - T_{return}$ ). If the aim is to supply the same amount of energy through the district network to the buildings, the mass flow needs to increase when the  $\Delta T$  reduces. Since the mass flow is directly proportional to the water velocity inside the pipes, the previous statement represents a problem: the district network was designed as a 3<sup>rd</sup> generation system with one specific maximum water velocity. The maximum water velocity differs from system to system but it is in the range between 2.0 m/s and 2.5 m/s [25, p. 108] [26, p. 20]. Therefore, a reduction of the district network temperature means to overcome this threshold, which may cause hydraulic problems in pumps or pipes since the water inside the network flows at a higher velocity for which the network was designed.

Both the water velocity problem and the reduction of the return temperature are the mayor challenges for performing a district heating system transformation and something that is tried to solve in this master thesis.

## 2.4 The Carnot Toolbox

The Carnot Toolbox (Conventional And Renewable eNergy systems Optimization Toolbox) is a software for the MATLAB-Simulink environment [27]. The toolbox was developed by the Solar-Institute Jülich of the Fachhochschule Aachen in 1998 and it allows the simulation of thermal systems of both renewable and non renewable components. The version used in this master thesis is the 6.3.

The Carnot Toolbox has six main block-sets: *Sources*, *Storage*, *Hydraulics*, *Control*, *Loads* and *Weather*. In each of them different components are available for example, solar thermal or heat pumps in the source set, or pumps, pipes and flow diverters in the hydraulic set. Since Carnot is inside the Simulink framework, all components must be dragged and dropped to a main frame and then connected to each other to create more complex systems.

Same as Simulink, the Carnot Toolbox is designed to simulate dynamic systems. Since the weather data is in an hourly format, it makes sense to choose an hourly step time in a period of one year. However it is possible to choose a bigger time step by using a delay component. The reason why a dynamic software was selected

is because inputs variables such as radiation, demands or ambient temperature, and internal variables such as network temperature or mass flows have different values on every hour of the year and these values strongly determine the efficiency of the system and its components. Because of that a LTDH model needs to be dynamic in order to capture all these variations and represent reliably the general behaviour of the system, something that is not possible with a static model.

# Chapter 3

## Methodology

The methodology for performing this master thesis can be divided into four steps as is shown in Figure 3.1.

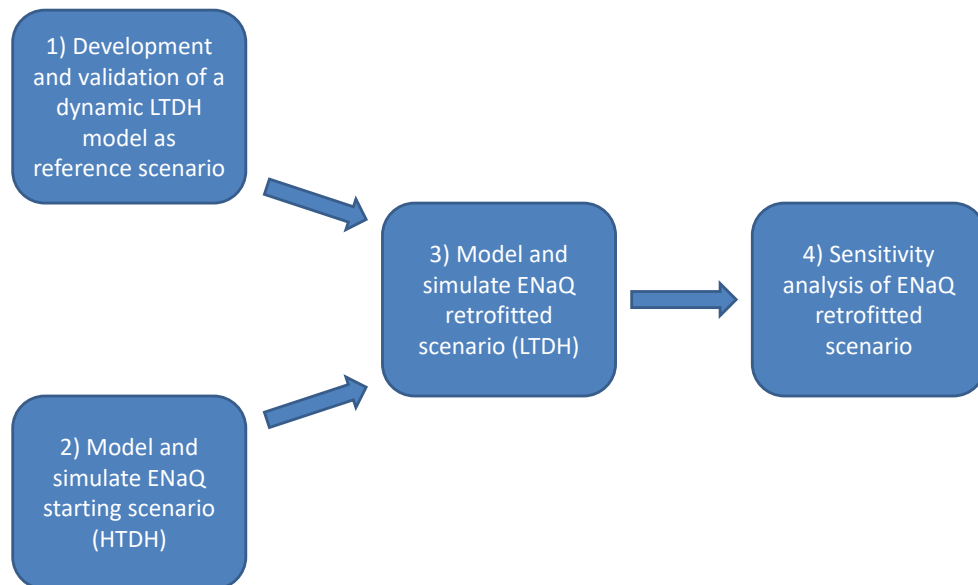


Figure 3.1: General overview of the methodology

The first step was to develop and validate a dynamic LTDH model to be used as a reference scenario. In order to do that, this master thesis was based on a study published in 2017 by the Technical University of Munich called “Potenziale von Niedrigtemperaturnetzen zur Steigerung des Anteils erneuerbarer Energien in

Quartieren”<sup>1</sup> [28] (from now on this study will be referenced as TUM). On this study a highly detailed model for implementing a LTDH was developed by coupling different software (Excel, TRNSYS and Dymola). On this master thesis, and with the Carnot Toolbox a LTDH model was simulated based on the data provided by the Technical University of Munich. As the Carnot Toolbox is not as powerful as the software combination used on the original study some simplifications were required but always being carefully of not loose generality. After modeling the LTDH a functional validation was carried out to assure the Carnot Toolbox model represent a LTDH system well enough.

The second step of this study was to model ENaQ as a HTDH i.e. **ENaQ starting scenario** which is the starting point of the district heating system transformation (see Figure 1.1). The third step to perform this master thesis was model **ENaQ retrofitted scenario**. This means take from one side the building technology, district network representation and seasonal storage of the validate reference case of LTDH and from other side the network topology, demands and weather data from the ENaQ HTDH and merge them to obtain the desired scenario. Also on this step key performance indicators (KPI) were defined to compare both high and low temperature district heating systems.

Finally a sensitivity analysis took place where the size of collector area and storage tanks were changed in order to see the performance of the system in case there are economic or space constrains that do not allow the implementation of the LTDH scenario.

### 3.1 Develop and validation of a dynamic LTDH model as reference scenario

As said before, the first step was to have a validated model for LTDH system in order to simulate ENaQ as one. The TUM study [28] is one example of how the system on each building and the district network could work. In this study, described in subsection 3.1.1, a low temperature district heating system was modeled by coupling different software that allow to simulate all the 16 buildings of the system. Since the Carnot Toolbox is not powerful enough to simulate all of the 16 buildings, it was decided to model only one building and then scale it up to represent the whole district. Thus, the Carnot Toolbox model can be divided into two main sections.

---

<sup>1</sup>In English: Potential of low temperature district heating systems to increase the share of renewable energy in neighborhoods



From one side there is the one building model, presented in subsection 3.1.2. On the other hand, in subsection 3.1.3 a method to scale up the system demands and also a method to represent the entire network in a two single pipes system, is described. Once the Carnot Toolbox model is described, its results were compared with the TUM ones in subsection 3.1.4.

### 3.1.1 Reference case: TUM study

In this study a low temperature district heating system was simulated by coupling the software Excel, TRNSYS and Dymola. As is shown in Figure 3.2, on the simulation, an Excel macro is used to model the demands (SH and DHW) of each building which then go to the TRNSYS software to simulate the building technology also for each building. After doing that and with the help of a software coupling tool called Building Controls Virtual Test Bed (BCVTB) each TRNSYS building was coupled with the network modeled in Dymola.

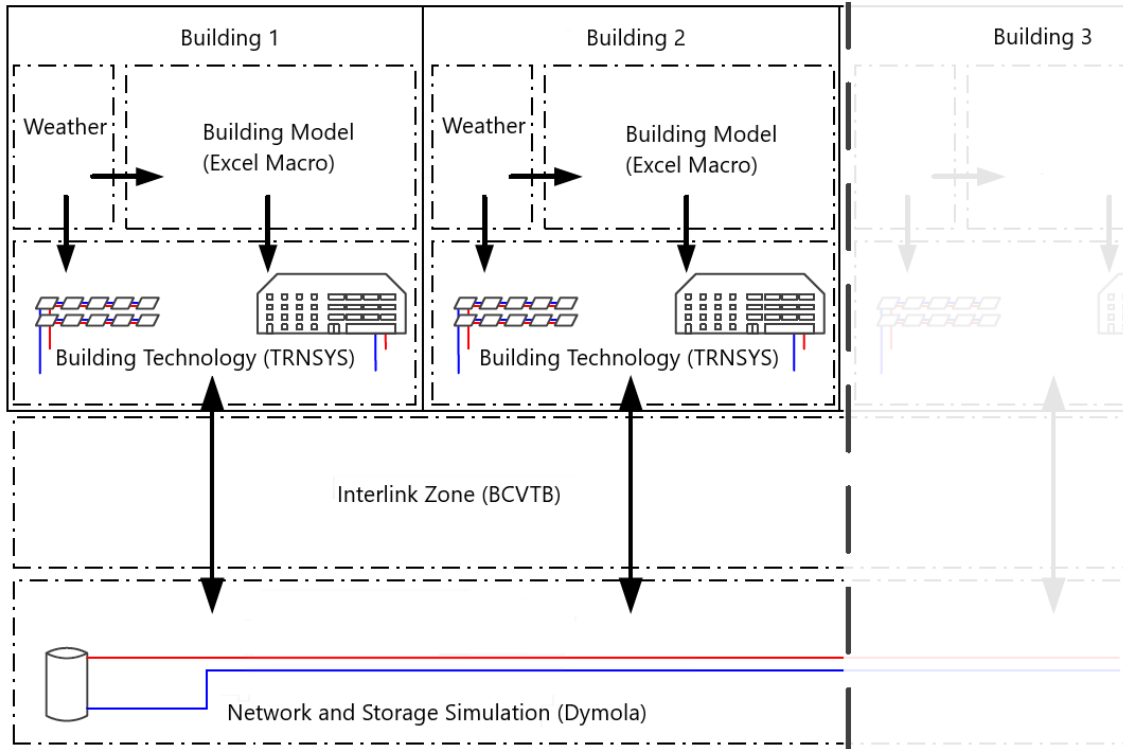


Figure 3.2: Software coupling of the TUM model (Figure translated from [28, p. 15])

The building technology system developed by the TUM is shown in Figure 3.3.

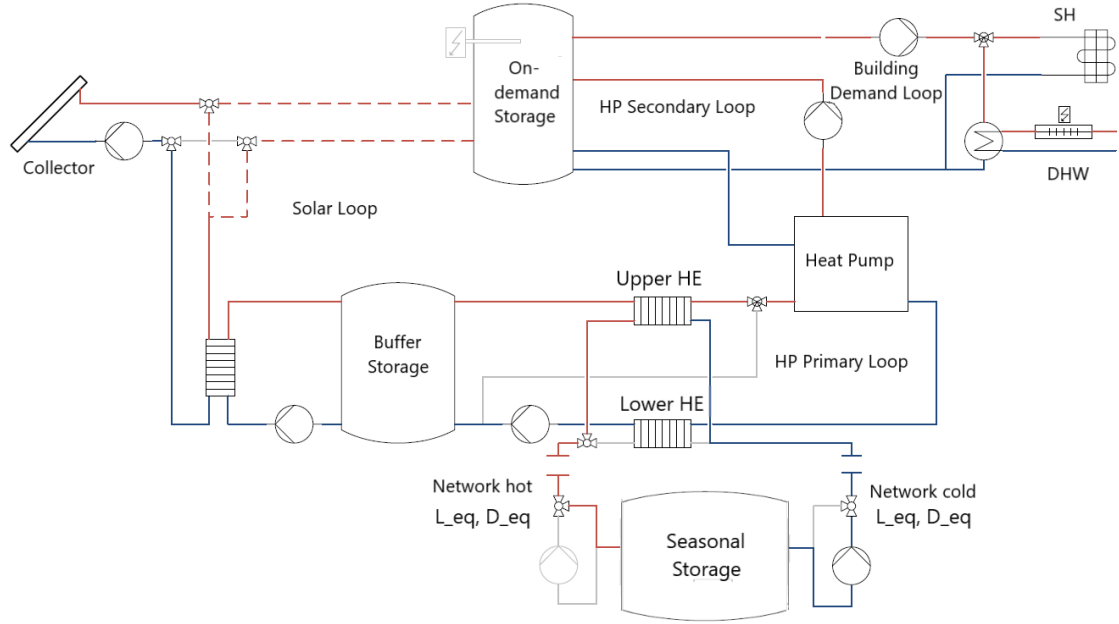


Figure 3.3: Building technology system of the reference scenario (Figure translated from [28, p. 19])

The scheme shows the technology of one building and the connection to the centralized seasonal storage through the network where all the other buildings with the same system are also connected. As it can be observed, the hydraulic system of each building is complex but it can be summarized into the following 7 points:

1. The connection between the heating system and the demands is done via the on-demand storage, which is always supplied by different technologies (solar collector, heat pump or electrical resistor) in order to keep the upper tank temperature between 40°C and 50°C. In case the DHW demand requires a higher temperature, an electrical water heater is at the outlet of the demand to raise the temperature.
2. The on-demand storage receives energy from the solar collectors if they reach a temperature of 50°C. If this is not the case, the heat pump supplies energy at 45,5°C using the buffer storage as the source side. If the temperature inside the on-demand storage is not enough, an electrical resistor inside the on-demand storage turns on and supplies heat until the temperature requirements are fulfilled.
3. The solar collectors work in two different modes. If the outlet temperature reaches 50°C, it supplies the energy directly to the on-demand storage. If

the collector gains energy but it is not enough to reach 50°C, then it supplies energy to the buffer storage by adjusting the mass flow to raise 10°C the inlet temperature.

4. The buffer storage is the connection point between the district network and the building technology. In winter it acts as a source for the heat pump by taking energy from the network or the collector when possible. In summer it gives energy to the network which is stored to be used in the winter period and also to stop the overheating of the building system.
5. The district network is a two pipes system which can change the direction of the mass flow according to a charging or discharging period. Therefore the upper heat exchanger is used when the building system gives energy to the network and the lower heat exchanger is used when the opposite process happens. Having this configuration requires always to have a hot and a cold pipe.
6. To avoid freezing or overheating the network, there are special control systems. In case the bottom part of the buffer storage reaches 4°C, the building is disconnected from the network. This leads to a cooling in the on-demand storage and consequently the activation of the electrical water heater. In case the network reaches 40°C, the building is also disconnected from the network. Then there is no more energy supply to the network and consequently no temperature rise.
7. For all buildings, SH demand is 24.4  $kWh/m^2a$  while DHW has a value of 30 l/person/day. Concerning the solar collector area (aperture) the design value is  $0.061 \frac{m^2_{collector}}{m^2_{living\ area}}$ . The two building storage tanks are sized according to the collector area with values of  $59 \frac{l}{m^2_{collector}}$  for the on-demand storage and  $118 \frac{l}{m^2_{collector}}$  for the buffer one.

The network model in Dymola consists on a bidirectional pipe system, where the direction of the flow changes depending on whether the seasonal storage tank acts as a source or sink. The length of the network is 915 meters which connects all the 16 buildings. The pipe modelling method is presented in Figure 3.4. Here the soil has a thermal inertia of 1.27  $kJ/kgK$  and also a conductivity of 1.8  $W/mK$ , while the insulation has a conductivity of 0.03  $W/mK$ . The soil temperature, modeled at a laying depth of 4  $m$  is simplified as a sinusoidal curve throughout the year, with a minimum of 2.2°C at the end of April and a maximum of 13.8°C at the end of October.

Finally the seasonal storage is a water tank<sup>2</sup> which has a volume of  $23000 \text{ m}^3$ .

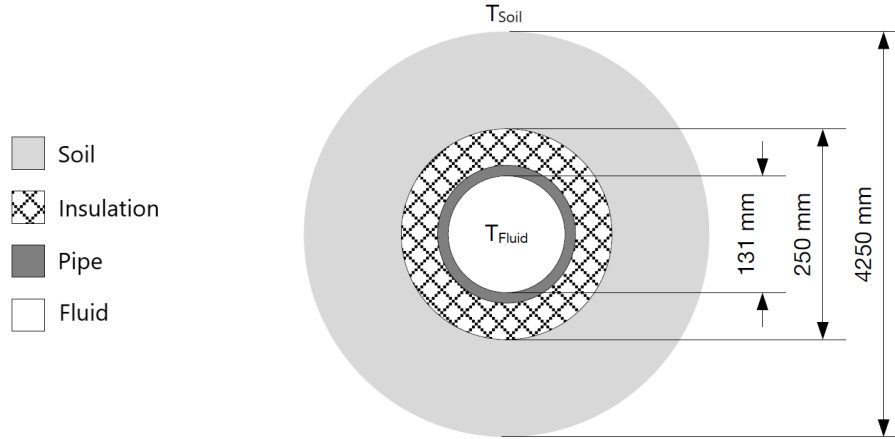


Figure 3.4: Pipe structure of the reference scenario (Figure translated from TUM [28, p. 28])

### 3.1.2 Single building model in the Carnot Toolbox

The single building model developed in this section corresponds to the TRNSYS part of the TUM study and it is presented in Figure 3.3. Before starting to describe how the system was modeled it is necessary to mention one change made in the Carnot Toolbox model compared to the TUM one. As mentioned in the theory, a reduction of the network temperature can only be achieved if the return temperature is reduced. To maximize this principle, the mass flow in the source side of the heat pump is always adjusted in order to have, if possible, an outlet temperature of  $4^\circ\text{C}$  returning to the buffer storage, always keeping in mind the mass flow range on which the heat pump works.

Having said that, the one building model can be divided into three main parts:

1. Solar collector loop
2. Building demands loop
3. Heat pump loop

Starting with the solar collector loop, since the Carnot Toolbox does not have a match flow pump component, it was necessary to develop a method to reproduce it. This method takes into account the heat gained in the previous time step and

<sup>2</sup>From the TUM study, the scenario 6 was taken as reference here, since it involves a water storage tank as seasonal storage and not a borehole storage as the ENaQ project geography does not allow a borehole heat storage

divides it by the desired  $\Delta T$  and the specific heat of the water. This mechanism also decides whether the energy is enough to reach 50°C and send the flow to the on-demand storage (OdS) or to raise the inlet temperature 10°C and send it to the buffer storage (BS). It is also important to mention that the weather data (solar direct and diffuse radiation as well as ambient temperature) was taken from the Carnot Toolbox data and corresponds to Stötten located in the federal state of Bavaria (Germany), where also the city of Munich is located.

Continuing with the building demands, one of the main components here is the on-demand storage (OdS) which is a 5 nodes water tank. This storage has different sensors on top and bottom of it to decide whether it is full in summer and the energy needs to go to the seasonal storage or if the energy provided from the solar collectors or the heat pump is not enough and needs an additional input from the electric water heater placed at the top of the tank which turns on when the upper temperature inside the tank falls below 36°C until it reaches a temperature of 40°C. The demand side was modeled exactly as the TUM was. There is only one pump for both SH and DHW. Then the route that the mass flow follows is decided by the diverted placed after the pump (see Figure 3.3). The demands were implemented with a constant inlet temperature and a variable mass flow which was calculated with the temperature difference ( $\Delta T=10^\circ\text{C}$  for SH and  $\Delta T=25^\circ\text{C}$  for DHW) and the power required each hour of the year provided by the TUM. Same as the reference case, the outlet temperature of DHW is set to be 45°C and 40°C for SH. For cases where the DHW outlet temperature is below 45°C, an electric water heater raises the temperature to the desired value.

The heat pump loop involves the heat pump, the buffer storage and the connection to the low temperature district heating system. Since the heat pump supplies energy to the on-demand storage always at 45.5°C, the match flow control strategy developed at the solar collector field, was used again but in this case, it was implemented not only at the sink side but also at the source side to reach, when possible, 4°C at the outlet of the source side too. The power curve of the heat pump was derived from the data sheet of it, which was provided by the TUM (see Annex A). The buffer storage is also a 5 nodes water tank. It has a temperature sensor on the top to decide when (23°C in summer and 31°C in winter) is necessary discharge it into the network and another one on the bottom to decide when is necessary to charge it from the network. The discharging process occurs through the upper heat exchanger and the charging through the lower one. Finally, same as the TUM model, there is an anti freezing sensor which disconnects the building from the network when the

temperature at the bottom of the buffer storage reaches 4°C.

In Annex B, images of the Carnot Toolbox model divided into these three main parts plus the district network are presented.

### **3.1.3 Scaling up method to represent the whole district heating system in the Carnot Toolbox**

The scaling up method to represent the whole district heating system developed in this section, corresponds to the Dymola part of the TUM study. Here not only the two pipes representation is addressed but also three other points which are important to explain first, in order to understand the method properly:

1. Scaling factor to represent the district demand
2. Bidirectional flow model
3. Pipes isolation parameter

Starting by the scaling up factor to represent the whole district system, as mentioned before, the one building model of Carnot Toolbox takes into account only one building but the district model takes into account the entire system. To be able to represent this, and knowing that the share of demand from the simulated building is 6% of the total district demand, the mass flow that goes from the building to the network is multiplied before entering to the network by 16.6 ( $= 0.06^{-1}$ ). In the same way the mass flow going from the network to the building is multiplied before entering to the building by 0.06. This assumption has as consequence that all buildings have the same demand profiles on every hour of the year and they are only scaled by how big is the area of each.

The second point to address is the bidirectional flow inside the pipes on the reference model. Dymola is able to change the direction of the mass flow, which means it can operate with only two pipes. The Carnot Toolbox is not able to do it. To cope with this problem a four line pipe system was implemented on the Carnot Toolbox but always only two pipes were considered for calculating the losses.

As is shown in Figure 3.5, there are two pipes for the charging and two for the discharging process. Each of them has a bypass to avoid the losses on the way to/from the seasonal storage. When the charging process is happening, only the charging pipes will be used and despite the simulation calculate the losses on the discharging pipes, the model does not take them into account since on this period the bypass on the discharging pipes is activated. The same logic applies when the

charging process happens. This method has as consequence that every time the mode is changed (charging/discharging), the initial pipe temperature is different, since the pipe itself is being changed. With this method, a two line pipe system can be represented with a four line pipe system.

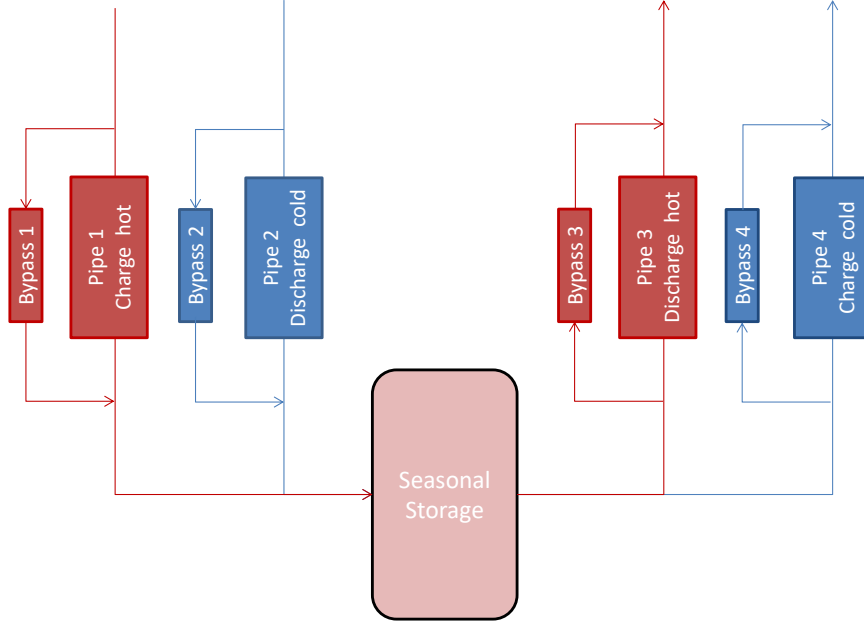


Figure 3.5: Scheme of the 4 pipes network modeled in the Carnot Toolbox

Regarding the insulation, on the reference case, as Figure 3.4 shows, there are two different insulation layers modeled, one corresponding to the insulation itself and another one representing the soil to consider the surroundings of the pipe. Because the pipe model in the Carnot Toolbox allows to consider only one insulation layer, it was necessary to calculate the equivalent thermal conductivity  $k_{eq}$  according to Equation 3.1.

$$\frac{1}{k_{eq}} \ln \frac{r_3}{r_1} = \frac{1}{k_1} \ln \frac{r_2}{r_1} + \frac{1}{k_2} \ln \frac{r_3}{r_2} \quad (3.1)$$

Where:

- $k_1$  = insulation conductivity of  $0.03 \text{ W/mK}$
- $k_2$  = soil conductivity of  $1.8 \text{ W/mK}$
- $r_1$  = pipe radius of  $0.0655 \text{ m}$
- $r_2$  = insulation radius of  $0.1250 \text{ m}$

- $r_3$  = soil radius of 2.1250  $m$

After clarifying these three points, the method for calculating the equivalent length and diameter of the network is described. As said before, in the Carnot Toolbox simulation only one building was taken into account but the energy circulating into the network is the one for the entire system. Hence it was necessary to use a method to estimate the losses in the whole network with a small amount of information:

- The lengths of each section of the network
- The demand share of each building
- The dimensions (inside and outside radius,  $r_{in}$  and  $r_{out}$ ) of the initial pipe (Figure 3.4)

In order to represent the network in a simple way with these conditions, it was necessary to impose 2 conditions:

1. The supply temperature in every section of the network is the same. That means that for every supply pipe the temperature difference between the section and the soil is the same. ( $\Delta T_{supply\ 1} = \Delta T_{supply\ 2} = \Delta T_{supply\ i} = \Delta T_{supply}$ ). The same principle applies for the return temperature of the district network.
2. The quotient between the outer radius and the inner radius is the same for all sections. ( $\frac{r_{out1}}{r_{in1}} = \frac{r_{out2}}{r_{in2}} = \frac{r_{out}}{r_{in}}$ ).

Based in these two conditions and looking at Equation 3.2 [24, p. 329] which represent the losses in one section, it is possible to calculate an equivalent heat transfer coefficient ( $U_{eq}$  [ $W/mK$ ]<sup>3</sup>) which is the same for all segments. After doing that, it is needed to multiply this  $U_{eq}$  with the sum of all the lengths of each section to represent the losses over the entire district network as Equation 3.3 shows.

$$Q_{loss} = \frac{2\pi k_{eq}}{\ln \frac{r_{out}}{r_{in}}} L \Delta T \quad (3.2)$$

$$Q_{loss} = U_{eq} \sum_i L_i \Delta T \quad (3.3)$$

Where:

- $k_{eq}$  = equivalent thermal conductivity [ $W/mK$ ]

---

<sup>3</sup>The units for  $U$  in a pipe are [ $W/mK$ ] and not [ $W/m^2K$ ] as in a wall are, is since here it is multiplied by the length of the pipe ( $L$  [ $m$ ]) while in a wall is multiplied by the area ( $A$  [ $m^2$ ]) of it.



- $r_{out}$  = outer radius of the pipe [m]
- $r_{in}$  = inner radius of the pipe [m]
- $\Delta T$  = temperature difference between the fluid inside and the soil outside the pipe [K]
- $L_i$  = length of each segment of the district network [m]
- $U_{eq}$  = equivalent heat transfer coefficient [W/mK]

The proposed method to represent the district network in one single pipe system is simple and accurate. However, it involves a very strong restriction such as the constant proportionality of insulation on every segment. In order to release this restriction, a generalization of the previous method was developed for cases when the insulation has not the same proportion on each segment which means calculate a new equivalent heat transfer unit  $U'_{eq}$  and a new equivalent length  $L'_{eq}$ .

### Equivalent length

Starting with the equivalent length, it was calculated following the method presented by Heimrath [29, p. 130]. Equation 3.4 shows how to calculate the equivalent length, where each  $L_i$  is each segment of the network where circulates a different mass flow  $\dot{m}_i$ . The calculation of each mass flow was based on the share of the demand of each building. This method was applied to the whole network in order to get the equivalent length  $L'_{eq}$ .

$$L'_{eq} = \frac{\sum L_i \dot{m}_i}{\sum \dot{m}_i} \quad (3.4)$$

### Equivalent heat transfer unit

For calculating this new  $U'_{eq}$ , the idea was to calculate every  $U_i$  for each segment since now every segment has a different  $U$  value. After doing this, it was only necessary to add each value to get the final  $U'_{eq}$  as Equation 3.5 and Equation 3.6 show.

$$U_i = \frac{2\pi k}{\ln \frac{r_{out\ i}}{r_{in\ i}}} \quad (3.5)$$

$$U'_{eq} = \sum U_i \quad (3.6)$$

The starting point for calculating every  $r_{in\ i}$  and  $r_{out\ i}$  was the bigger pipe which was provided by the TUM study so the values of  $r_{in1}$  and  $r_{out1}$  were known. For

calculating  $r_{in\ i}$ , the  $r_{in1}$  value was scaled according to the share of mass flow that circulates in the pipe  $i$ . For calculate  $r_{out\ i}$  there were two options and it depends on how the pipes in the network are insulated: with a constant thickness on every pipe or a variable one. In the first case,  $r_{out\ i}$  is  $r_{in\ i}$  plus a certain thickness and in the second one,  $r_{out\ i}$  is calculated to always maintain the ratio  $r_{in1}/r_{out1}$  (which leads to the simple method presented before).

On the Carnot Toolbox model, since there was no information provided by the TUM study about how the  $r_{out\ i}$  were designed, both methods were tested. The method with a proportional insulation showed much more similar results when calculating the losses, reaching 83.0% of the TUM losses (and as mentioned before and show in subsection 3.1.4, this difference is due to the match flow strategy at the heat pump and not because the pipe isolation model), while the method with constant isolation accounted for 59.8% of them. Therefore the constant  $\frac{r_{out}}{r_{in}}$  method was used on the Carnot model but with the  $U'_{eq}$  calculations. Summarizing this section, Equation 3.7 shows the method used on this study. It is important to remark, that to use the method as proposed here, the lengths of each segment must be of the same order of magnitude.

$$Q_{loss} = U'_{eq} L'_{eq} \Delta T \quad (3.7)$$

### 3.1.4 Functional validation of the Carnot Toolbox model

After a model on the Carnot Toolbox was developed and simulated the district heating system for one year, the results were taken and compared with the ones published by the Technical University of Munich.

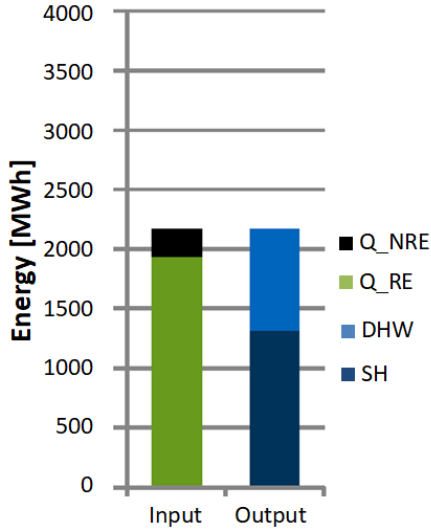
One general table and six different graphs cover all the edges of the simulation and all of them were compared with the Carnot Toolbox model. Results from both models are very similar and the all the important differences come from the same source: the solar radiation data from the Technical University of Munich model is higher than the one for the Carnot Toolbox model since the first one takes data from Munich and the second one from Stötten. That leads to a higher share of electrical power used on the Carnot Toolbox model since the demand for both models is the same. A possible solution to minimize this difference on the solar energy gained for each model would have been to increase the collector area of the Carnot Toolbox model but it was decided to keep the values that the TUM used in order to not distort the validation process.

Having said that Table 3.1 and Figure 3.6 show an overview of both models.

Table 3.1: Results comparison between TUM and Carnot Toolbox model: general overview

	<b>TUM</b>	<b>Carnot Toolbox</b>
<b>Total Energy [MWh]</b>	2166	2121
<b>Share of RE [MWh]</b>	1936 (89%)	1761 (83%)
<b>Share of NRE [MWh]</b>	230 (11%)	360 (17%)
<b>JAZ</b>	5.66	3.83

Technical University of Munich model



Carnot Toolbox model

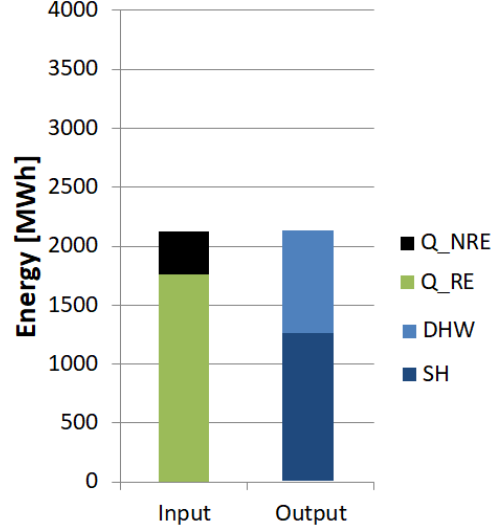


Figure 3.6: Results comparison between TUM (Figure translated from [28, p. 63]) and Carnot Toolbox model: General Overview

Observing the results, the final energy produced is the same but the share of not renewable energy<sup>4</sup> is higher on the Carnot Toolbox model, as said before due to the difference of radiation data on each model. To represent the amount of electrical energy used on the system the “Jahresarbeitszahl” (JAZ) was calculated. It is defined as Equation 3.8 shows and the higher the better because it means less use of electricity and therefore more use of renewable energy sources.

$$JAZ = \frac{\sum Q_{SH} + \sum Q_{DHW}}{\sum W_{el}} \quad (3.8)$$

<sup>4</sup>Both models assume a share of RE in the electric grid of 35.12%

The JAZ for both models are not the same. The JAZ for the Carnot Toolbox is almost 2/3 of the one for the Technical University of Munich. The explanation of this is because each model uses different radiation data. This difference causes that the amount of electricity used on the TUM model is almost 2/3 than the used in the Carnot Toolbox model and since the JAZ is inversely proportional to the electricity used, the JAZ from the Carnot Toolbox is 2/3 of the JAZ from the TUM model.

Figure 3.7 shows the energy produced and demand covered for each month in the year for the whole district.

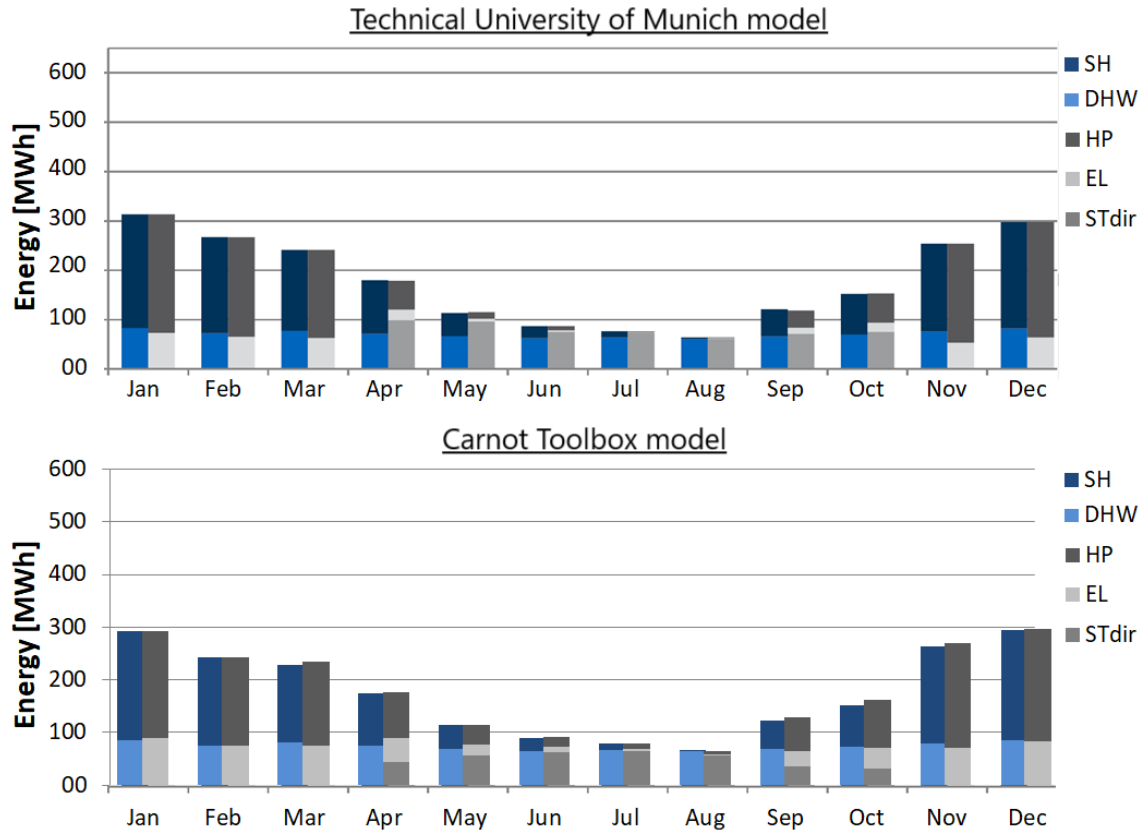


Figure 3.7: Results comparison between TUM (Figure translated from [28, p. 63]) and Carnot Toolbox model: Monthly shares of energy by source and demand covered

The energy produced is divided depending where the energy comes from: heat pump (HP), solar thermal direct ( $ST_{dir}$ ) and electricity (EL) whereas the demand covered is divided into space heating (SH) and domestic hot water (DHW). Here it is possible to see how the DHW demand is almost constant throughout the year while SH demand is considerable high in winter and nearly zero in summer. In winter the energy is generated by the heat pump, using the heat stored in the seasonal storage and the electrical water heating (the auxiliary inside the on-demand storage and the one at the DHW outlet). In summer the energy is mainly generated by the solar

collectors located on the rooftops of each building. On the Carnot Toolbox model, there is a share of energy in summer that is still generated by electricity, whereas on the TUM model it is not the case. As said before, the lack of energy due to a lower solar radiation leads to this difference. Despite the mentioned difference, both models show a clear the same trend not only because of where the energy comes from but also on how much energy is generated by each source.

Figure 3.8 shows the monthly energy balance between all the buildings and the seasonal storage.

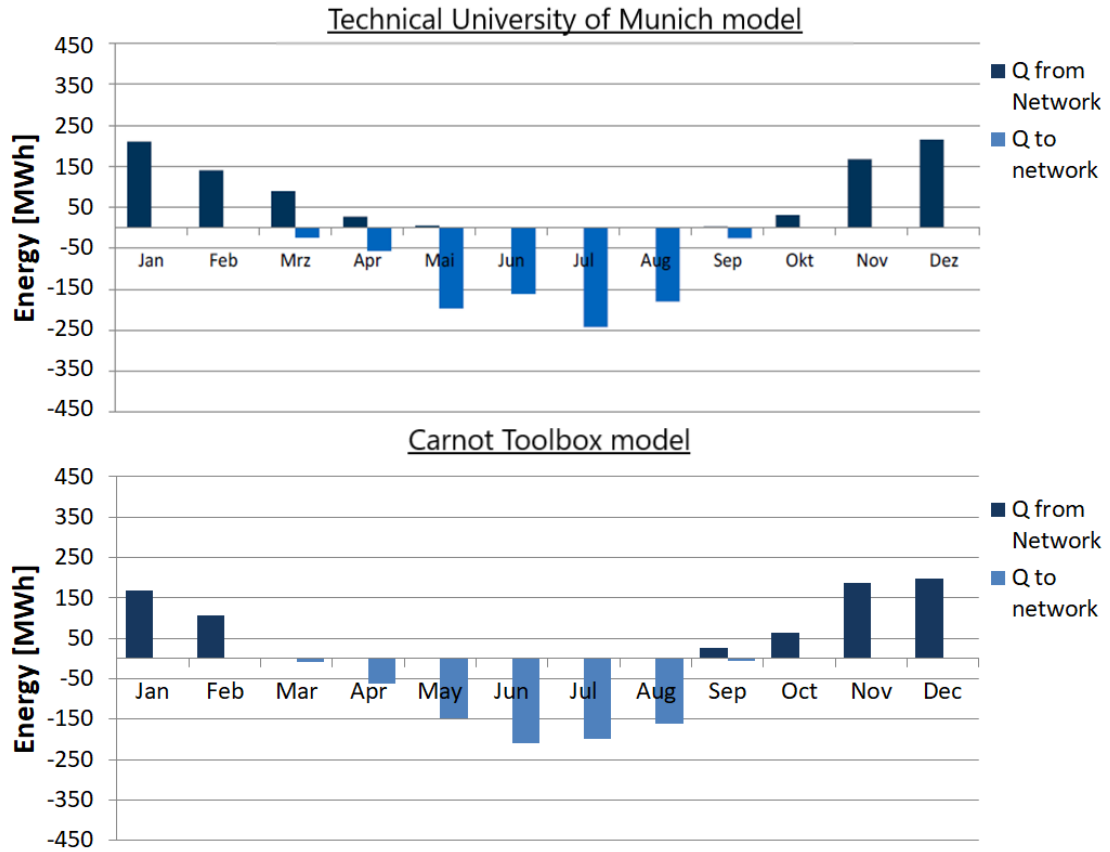


Figure 3.8: Results comparison between TUM (Figure translated from [28, p. 64]) and Carnot Toolbox model: Monthly energy balance between the district network and the seasonal storage

Because in summer the radiation is higher, and on each building there are solar collectors gaining energy, the buildings give energy to the seasonal storage tank (charging process), while in winter they take energy from it (discharging process). One difference between both models occur in March: while the TUM model is still in a discharging process, on the Carnot Toolbox model the storage is empty. This happens because in summer, the TUM model gives more energy to the seasonal storage (overcoming 150 *MWh* on each month from May until August and almost

reaching 250 *MWh* in July) and therefore it can take more energy in winter while the Carnot Toolbox model (reaching 150 *MWh* in June, July and August) can not do this because of less radiation. Nevertheless, it is important to remark that the yearly energy balance of the seasonal storage in both models is zero, so there is neither a surplus nor a lack of energy on the system.

Figure 3.9 shows the network temperature for the TUM and Carnot Toolbox model.

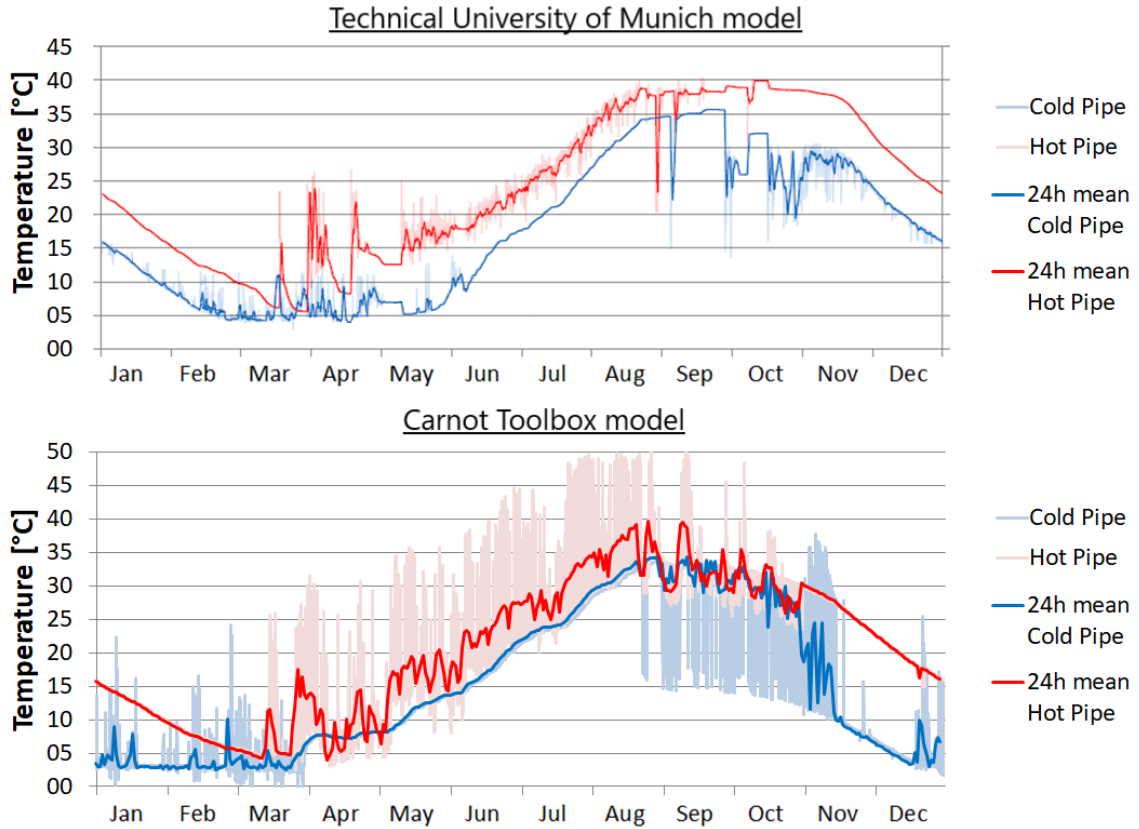


Figure 3.9: Results comparison between TUM (Figure translated from [28, p. 64]) and Carnot Toolbox model: Network temperature

The red line represents the hot pipe and the blue the cold one. The transparent lines represent the hourly temperature and the thick ones indicates the daily average (24h). The overall behaviour on both model has the same trend: from December until March the temperature decreases since the seasonal storage is getting empty while in summer, from April until August, the temperature increases when the buildings give energy to the seasonal storage. There are three main differences when comparing the results of both models.

First, in months December, January and February the cold pipe temperature decreases in the TUM model, from 16°C to 4°C, while in the Carnot Toolbox model it maintains a value of 4°C in almost the whole period. This difference occurs because

the change made in the Carnot Toolbox mentioned in subsection 3.1.2 where the outlet of the heat pump tries always to reach 4°C.

Second, the hourly values for the Carnot Toolbox model have a bigger range than the ones presented in the TUM model. The reason of this is because the Carnot Toolbox model uses only one building as reference and then scales it up to emulate the whole district whereas the TUM model simulate each of the buildings. This means that all the heat transfer processes between the buildings and the district network happen at the same time and the same point in the Carnot Toolbox while it happen at 16 different points and at different times in the TUM model, making in theory, the energy changes 16 times bigger in the Carnot Toolbox, which can be seen in these temperature changes. Because of this issue, from now onwards the temperature parameter that will be used to compare both models will be the 24h average since this value gives the Carnot Toolbox enough time to buffer the mentioned problem.

The third difference lies in months September and October. The TUM model reaches 40°C and therefore the seasonal storage is disconnected from the buildings causing a stagnation of the temperature on the network as long as the buildings do not require a big energy input from the storage (from middle October) In these two months, each building is able to supply their heat demands with the solar collectors, something that is not possible in the Carnot Toolbox model because of less solar radiation. That explains why the 24 hours average temperature in the Carnot Toolbox model starts to decrease in September. Having less radiation in summer also implies that the temperature reached in the charging period is not so high as the TUM model, and consequently never disconnect the seasonal storage from the buildings for larger periods.

Figure 3.10 shows the total district network losses on each month. Since the losses are a direct function of the network temperature, the higher the temperature, the higher the losses.

Here again, both models show almost the same trend on each month except for when the temperatures on each model are different: from one side December, January and February where the Carnot Toolbox losses are less because of the outlet temperature of the heat pump. Indeed, the losses in January and February are negative which means gains in the pipes because of the low temperature inside of them. From the other side in months September and October where the TUM model have less losses. The reason why the TUM model have less losses on these two months is because, as said before, the disconnection of the district system from the buildings.

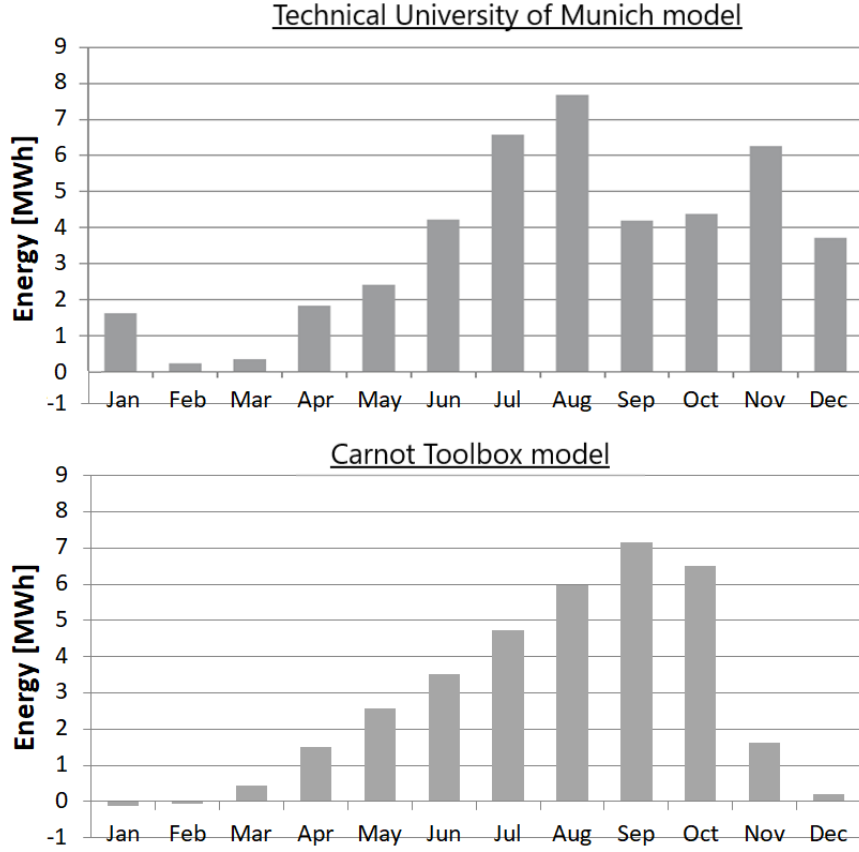
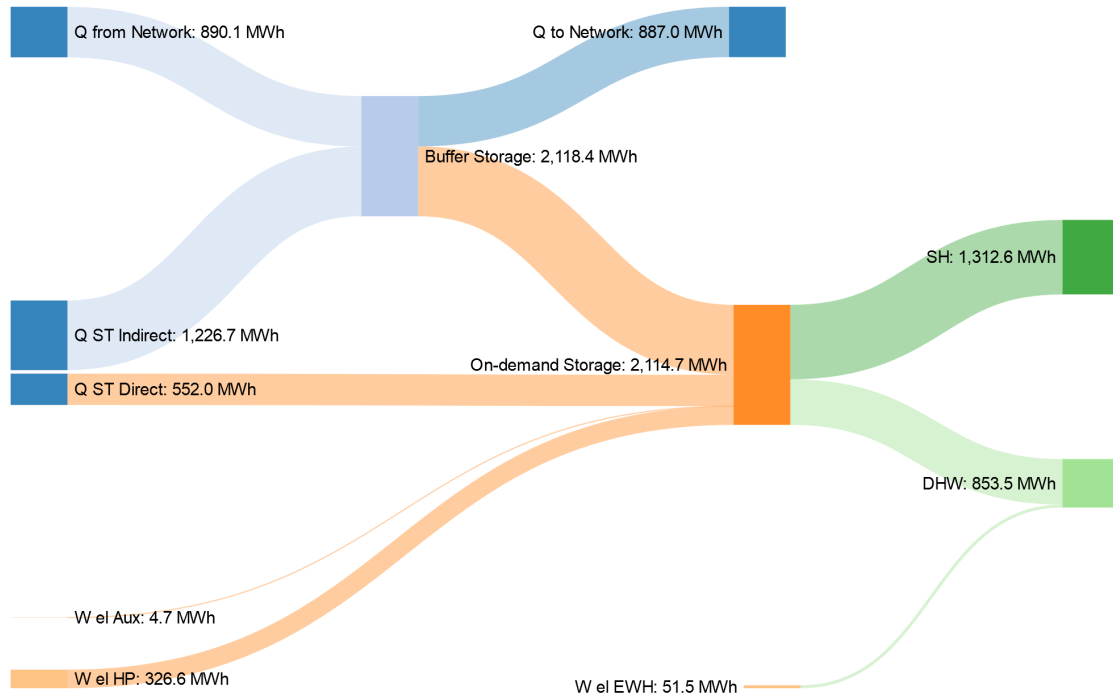


Figure 3.10: Results comparison between TUM (Figure translated from [28, p. 65]) and Carnot Toolbox model: Monthly losses in the district network

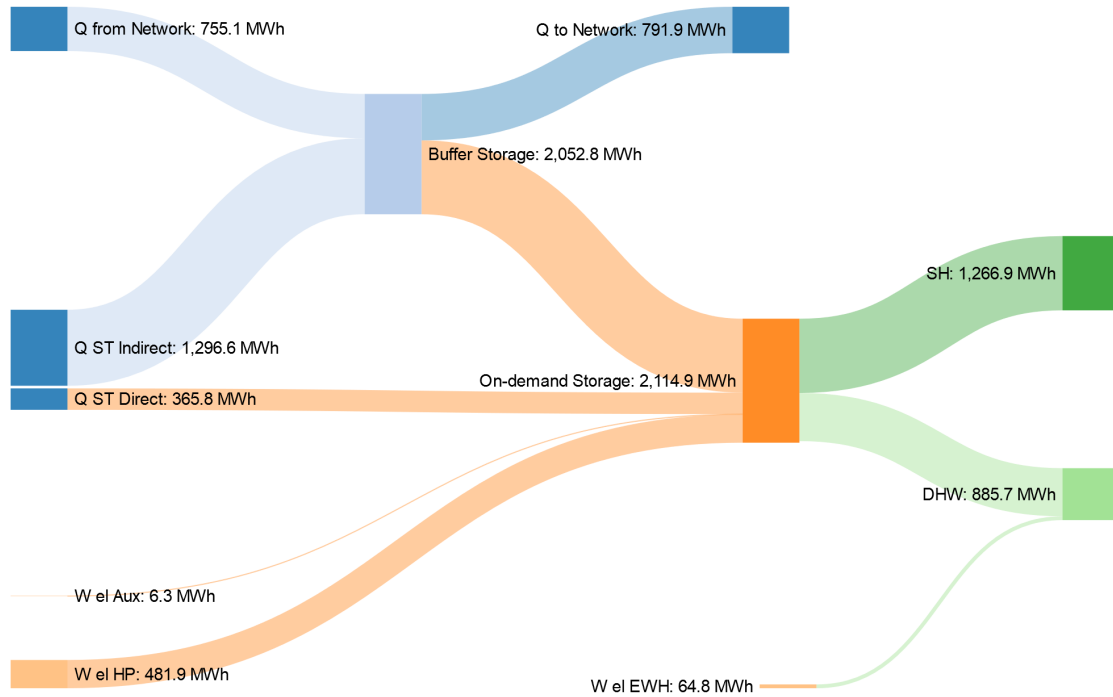
When this disconnection occurs, there is no flow inside the pipes, which following the convection heat transfer mechanisms, leads to less losses in comparison when there is a flow inside of the pipes as the Carnot Toolbox model is.

The last comparison point between both models is the Sankey diagram presented in Figure 3.11. The left boxes of each diagram represent the sources for producing energy: network (seasonal storage), solar thermal direct to the on-demand storage or indirect to the buffer storage and electricity either for the heat pump or the auxiliary heater inside the on-demand storage or the electric water heater which rise the temperature of the DHW when necessary. On the right side are the demands: space heating and domestic hot water. There is also the network (seasonal storage) as a sink for giving energy in summer. To complete the description, in the center of both diagrams there are the buffer and on-demand storage.





(a) Technical University of Munich model



(b) Carnot Toolbox model

Figure 3.11: Results comparison between TUM and Carnot Toolbox model: Sankey diagram

Based on the Sankey diagrams, table 3.2 shows the % of energy generated by source for both models. Similarly, Table 3.3 shows where the energy is sank . The mayor difference is in the solar energy that goes directly to the on-demand storage (Q ST Direct) which is 5.8% (187 *MWh*) more in the TUM model. The reason for having such a difference lies, as mentioned before, in the different solar radiation that each model has. This lack of energy in the Carnot Toolbox model, is covered with electricity on the heat pump. The second difference appears in the energy taken from network, with 3.8% more in the TUM model. The reason of this difference is because there is less energy sent to the storage because the radiation data. This phenomenon can also be observed on the energy sent to the network where again, the Carnot Toolbox sends less energy than the TUM model.

Table 3.2: Share of heat sources for TUM and Carnot Toolbox

Source	TUM Supply [%]	Carnot Toolbox Supply [%]
Q from Network	29.1	25.3
Q ST Indirect	40.2	43.5
Q ST Direct	18.1	12.3
W el Aux	0.2	0.2
W el HP	10.7	16.6
W el EWH	1.7	2.1
Total	100	100

Table 3.3: Share of heat sinks for TUM and Carnot Toolbox

Sink	TUM Demand [%]	Carnot Toolbox Demand [%]
Q to Network	29.1	26.9
SH	43.0	43.0
DHW	28.0	30.1
Total	100	100

After comparing different parameters and graphics, the conclusion of this section is that the Carnot Toolbox model represents the Technical University of Munich model in a suitable way. There is no model 100% equal to another but here, after reviewing 6 different graphics (from Figure 3.6 to 3.11) and 3 tables (from Table 3.1 to 3.3) all of the main trends behaves in the same way.

From now on wards, this Carnot Toolbox model will be used as the reference scenario for how a low temperature district heating system should be.

### 3.2 Model ENaQ starting scenario (HTDH)

After having a validated model for the aiming scenario, the starting point was modeled, which means ENaQ as a HTDH. Before modeling this scenario, it is necessary to know two key aspects of the neighborhood: the network topology and the demands.

Starting with the topology of the network, Figure 3.12 shows the projected system on the ENaQ project<sup>5</sup>. There are seven buildings in the neighborhood with one connection for each of them. The project also incorporates an energy center<sup>6</sup> where the energy system of the neighborhood is monitored. Inside this energy center, the blue dot represents the centralized CHP unit of the district heating system.

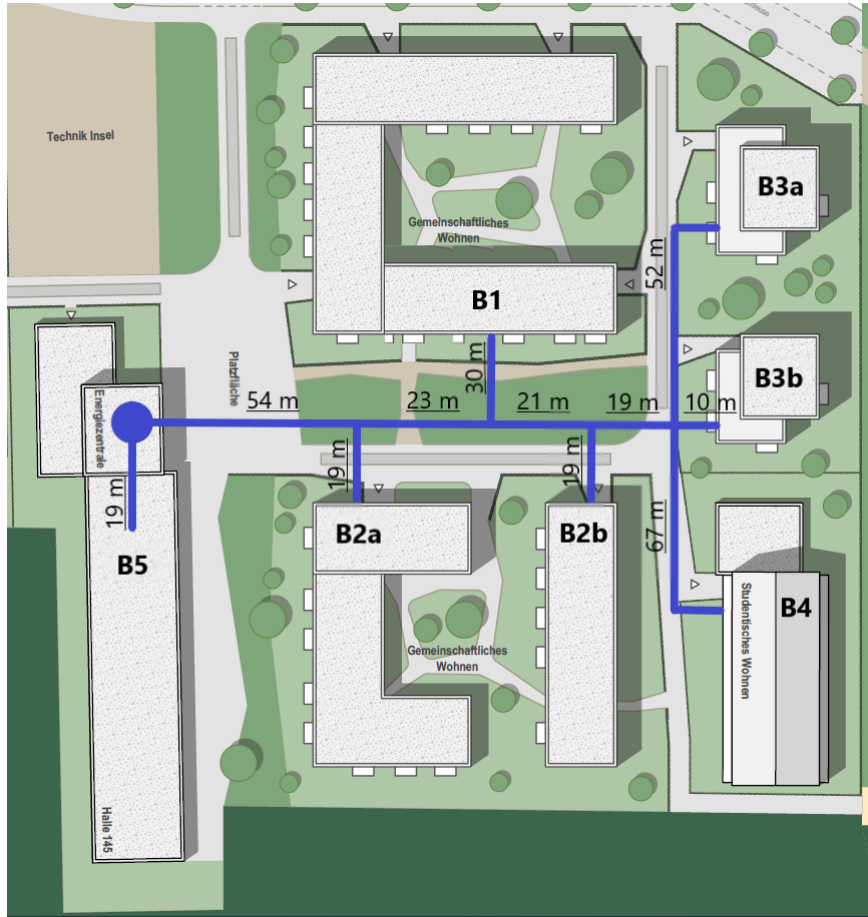


Figure 3.12: ENaQ district heating system (Figure obtained from GSG company)

Buildings 1 to 3b are residential buildings for multi family houses, while building 4 is a student house. The building 5 is a hall where a canteen and some apartments are. In total the district network has a length of 454 m. With the experience gained by

<sup>5</sup>The building plan is property of GSG company and was proposed in April 2020

<sup>6</sup>Energiezentrale in the draft

simulating and validating the LTDH reference model in subsection 3.1, the method described in subsubsection 3.1.3 was used in order to simulate the whole network in a two pipes system resulting an equivalent length of  $L_{eq} = 41.12 \text{ m}$  and an equivalent heat transfer unit of  $U_{eq} = 3.53 \text{ W/mK}$ .

Continuing with the ENaQ demands, for the multi family houses, an annual value of around  $30 \text{ kWh/m}^2\text{a}$  was used for SH. For the student house this value rises until  $36.4 \text{ kWh/m}^2\text{a}$  and for building 5 it is  $117.8 \text{ kWh/m}^2\text{a}$ . The DHW demand has an annual value of  $12 \text{ kWh/m}^2\text{a}$  for all buildings. Table 3.4 shows the area, SH and DHW specific demand, the total demand and the share of it for each building.

Table 3.4: Area, SH and DHW specific demand for each building in ENaQ project

	Area [ $\text{m}^2$ ]	SH demand [ $\text{kWh/m}^2\text{a}$ ]	DHW demand [ $\text{kWh/m}^2\text{a}$ ]
<b>B1</b>	3215	29.5	12.5
<b>B2a</b>	1942	30.4	12.5
<b>B2b</b>	1092	29.4	12.5
<b>B3a</b>	1037	25.8	12.5
<b>B3b</b>	890	26.3	12.5
<b>B4</b>	2054	36.4	12.5
<b>B5</b>	1112	117.8	12.5

With this data, hourly profiles for SH and DHW were generated for each building. According to the district scaling method, building 3b was selected to be the reference building because it is the building which has the highest peak loads per square meter. Since the scaling up method is done with respect to the area of each building, when the B3b peak load occurs, then all buildings will have the maximal peak load their area allows them to have, something very unlikely to happen (that all buildings have their peak load at the same moment of the year). However by doing this, the district demand representation is always in the safer side where it is sure there will not be a higher peak load than the one calculated by this method.

With these two aspects clear, Figure 3.13 shows a scheme of the HTDH model. On the left there are the CHP unit with a centralized storage for cases when the CHP is not running. Then comes the district network and finally the demands. On the demand side, there is an electric water heater at the outlet of the DHW for specific cases where the supply system is not enough. It is important to point that in the real project, the CHP unit has a thermal output of  $100 \text{ kW}_{th}$  and there is a gas boiler as a back up with a thermal output of  $420 \text{ kW}_{th}$  which is the highest peak load of the system in winter. Nevertheless for this model it does not make any difference since

both technologies supply water at  $80^{\circ}\text{C}$  and have a thermal efficiency of  $94.2\%$ <sup>7</sup>. The centralized storage has a size of  $9\text{ m}^3$  [30] with ten nodes and the control strategy is adjusted for turning the CHP (or gas boiler) on when the temperature of the upper node falls below  $70^{\circ}\text{C}$  until this temperature reaches  $80^{\circ}\text{C}$  again.

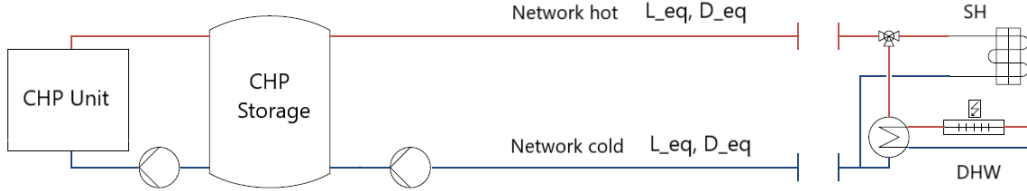


Figure 3.13: Scheme of ENaQ HTDH

### 3.3 Model ENaQ retrofitted scenario (LTDH)

With a validated model of a LTDH system and the demands and network topology of the ENaQ neighborhood, it was possible to model ENaQ as a LTDH. For doing this apart from taking the network and demand from ENaQ HTDH, and merged them into the LTDH model, the weather data had to be changed, since ENaQ is not located in Stötten as the validation model was placed.

Temperature and radiation hourly profiles corresponding to Oldenburg were used. The average temperature is  $10^{\circ}\text{C}$  with a maximum of  $32^{\circ}\text{C}$  on August 25<sup>th</sup> and a minimum of  $-10^{\circ}\text{C}$  on January 20<sup>th</sup>. The radiation received in Oldenburg is  $1033.8\text{ kWh/m}^2\text{a}$  with a maximum of  $0.911\text{ kWh}$  on June 19<sup>th</sup>. The radiation can also be divided into direct and diffuse where the first one accounts for  $463.5\text{ kWh/m}^2\text{a}$  while indirect is  $570.3\text{ kWh/m}^2\text{a}$ .

For performing the district heating system transformation, it was decided to place the seasonal water storage tank in the energy center where the CHP previously was. The volume of the tank was scaled from the TUM model and has a value of  $6198\text{ m}^3$ . Same as the ENaQ HTDH model, building 3b was selected as reference building. With the area of building 3b, the size of the collector field was scaled and then the

<sup>7</sup>The thermal efficiency was calculated based only on the thermal part of the CHP which means removing the fuel used to generate electricity (The nominal values are:  $177\text{ kW}$  of natural gas produce  $67\text{ kW}_{el}$  and  $100\text{ kW}_{th}$ )

size of the buffer and on-demand storage according to the reference case parameters. These values are shown in Table 3.5.

Table 3.5: Solar collector area, buffer and on-demand storage sizes for building 3b

	Reference case relation	Building 3b value
<b>Solar collector area</b>	$0.061 \text{ m}^2/\text{m}_{\text{living area}}^2$	$54 \text{ m}^2$
<b>Buffer storage size</b>	$118 \text{ l}/\text{m}_{\text{coll}}^2$	$6372 \text{ l}$
<b>On-demand storage size</b>	$59 \text{ l}/\text{m}_{\text{coll}}^2$	$3186 \text{ l}$

To finalize the modeling process the network water velocity constrain had to be implemented (see Section 2.3) and the network temperature constrain had to be released. Starting with the water velocity constrain, the original network i.e. **ENaQ starting scenario** was designed in order to have a maximal network water velocity of  $2.5 \text{ m/s}$  which was done by limiting the mass flow of the district network pump. Because the network used in **ENaQ retrofitted scenario** is the same, then the same condition needs to be applied. Therefore an extra constrain was implemented in the model that does not allow water to have velocities higher than  $2.5 \text{ m/s}$ . Regarding the network temperature constrain, in the reference LTDH model, there is a maximal temperature allowed in the network of  $40^\circ\text{C}$ . Again, because the original network was designed for a HTDH, this LTDH constrain was released now to cut the supply when the network temperature reaches  $80^\circ\text{C}$ .

### 3.4 Development of key performance indicators to compare different scenarios

Once **ENaQ starting scenario** and **ENaQ retrofitted scenario** were modeled and simulated it is necessary to have suitable tools to compare them. Under this line, key performance indicators (from now on wards KPI) were developed for such a comparison.

Five KPI were developed in order to cover all the edges of both district heating systems and are presented below:

1. **Share of renewable energy sources [%]**: This indicator shows how much energy respect to the covered demand, comes from renewable sources. Here it is important to mention that when energy from the electrical grid is taken, this indicator assumes that it comes with a renewable energy share of 35% as the TUM study does. Also important is to mention that the CHP works with

natural gas and has a thermal efficiency of 94.2% (see subsection 3.13).

2. **Share of electricity used in the system [%]**: This indicator shows how much energy respect to the covered demand, comes from the electrical grid. Electricity is used in heat pumps or electric water heaters. The idea behind this indicator is to show the power-to-heat relation in the system.
3. **Energy taken from the district network [%]**: This indicator shows how much energy respect to the covered demand, is taken from the district network. The idea behind this indicator is to show how much centralized or decentralized energy sources does the system have.
4. **Transport losses [%]**: This indicator shows how much energy, from the whole energy produced, is lost. Here is important to mention the difference between supplied energy and transported energy. The first one is the energy that only goes from the CHP/seasonal storage tank to the system while the transported energy is the energy sent from or to the CHP/seasonal storage. In a system without a seasonal storage, the supplied energy coincides whit the transported energy. However in a system with a seasonal storage the transported energy is always bigger than the supplied since there is energy sent to the seasonal storage and energy taken from it in different periods of the year.
5. **GHG emissions [tCO<sub>2</sub>eq]**: This indicator, one of the most important, shows the emissions that the district heating system produces. Here it is important to mention that in this study, emissions for natural gas were considered as 200 *g/kWh* [31, p. 41] and for the electrical grid 401 *g/kWh* [32].

### 3.5 Sensitivity analysis of ENaQ retrofitted scenario

When observing the amount of technologies that must be implemented in the **ENaQ starting scenario** to transform it into **ENaQ retrofitted scenario** for each building they are not few: three heat sources (solar collectors, heat pumps and electrical water heaters), two heat storage tanks, three heat exchangers, four water pumps, apart from pipe connections and valves.

Performing this system transformation in a software is not so challenging, since it involves adding more components and removing other ones from the HTDH system. However, in the real life there are always economic and, in this case, also space constrains which may not allow this transformation to happen.

Under this point of view there are three main technology implementations that may restrict the district heating system transformation:

1. The size of solar collector field
2. The size of the seasonal storage tank
3. The possibility of installing only one decentralized storage on each building

These technology implementations were categorized into two groups. From one side there is the size variation at the solar collector field and at the seasonal storage tank, since there is a strong relation between these two variables. On the other hand, there is the possibility of install only one decentralized storage on each building. These two groups were studied in two different sensitivity analysis.

### **3.5.1 ENaQ retrofitted with different solar collector area and different seasonal storage volume**

In this sub sensitivity analysis, different scenarios were simulated when either the solar collector area or the seasonal storage volume were different as the reference case (**ENaQ retrofitted scenario**). In order to have the whole spectrum of how these variables behave, it was decided to create a matrix of scenarios where on the horizontal axis the seasonal storage volume changes and on the vertical axis the size of the solar collector field changes. It was also decided not only simulate scenarios where the size of these variables is lower than the reference case but also when it is higher. With all this in mind, scenarios were simulated where the size of these variables were in the range from 0.4 until 1.4 of the reference case with a step of 0.2.

After each simulation, all five KPI were calculated for each scenario so at the end, five heat maps were developed.

### **3.5.2 ENaQ retrofitted with only one decentralized storage**

The second part of the sensibility analysis deals with covering the possibility of having only one decentralized storage tank for each building. Removing the on-demand storage tank is not possible because there should always be the option of having hot water available if necessary. However it is worth asking how the system performs without the buffer storage.

To do this, it was necessary to reconfigure the heat pump primary loop since now this loop is directly connected with the solar loop. The reconfiguration consists of a decoupling between the heat pump primary loop and the connection to the district





# Chapter 4

## Results and Discussion

On this section, results of the process described on Chapter 3 are shown and discussed. This means the comparison between **ENaQ starting scenario** and **ENaQ retrofitted scenario**, and the sensitivity analysis of this last one. Since the results of the modeling and validation process of a reference case for a LTDH were shown in Chapter 3 and they do not belong directly to the ENaQ project, they will not be shown here again. The structure of this Chapter is organized as follows: results are always shown with charts followed by bullet points which describe the most important remarks. After that, the discussion of the results comes in a paragraph format.

### 4.1 Comparison between ENaQ starting (HTDH) and ENaQ retrofitted (LTDH) scenario

As the title of this master thesis mentions, the first comparison between both scenarios involves the temperature of the district heating system. Figure 4.1 shows the **ENaQ starting scenario** temperature for one year in an hourly time step. Same as the validation process chart (Figure 3.9), the red line represents the hot pipe while the blue line represents the cold one. There are also a light and a dark line to represent the hourly and the 24h mean values respectively. As mentioned in subsection 3.1.4 the analysis is based on the 24h mean temperature since the hourly values are influenced by the scaling up process in the Carnot Toolbox model.

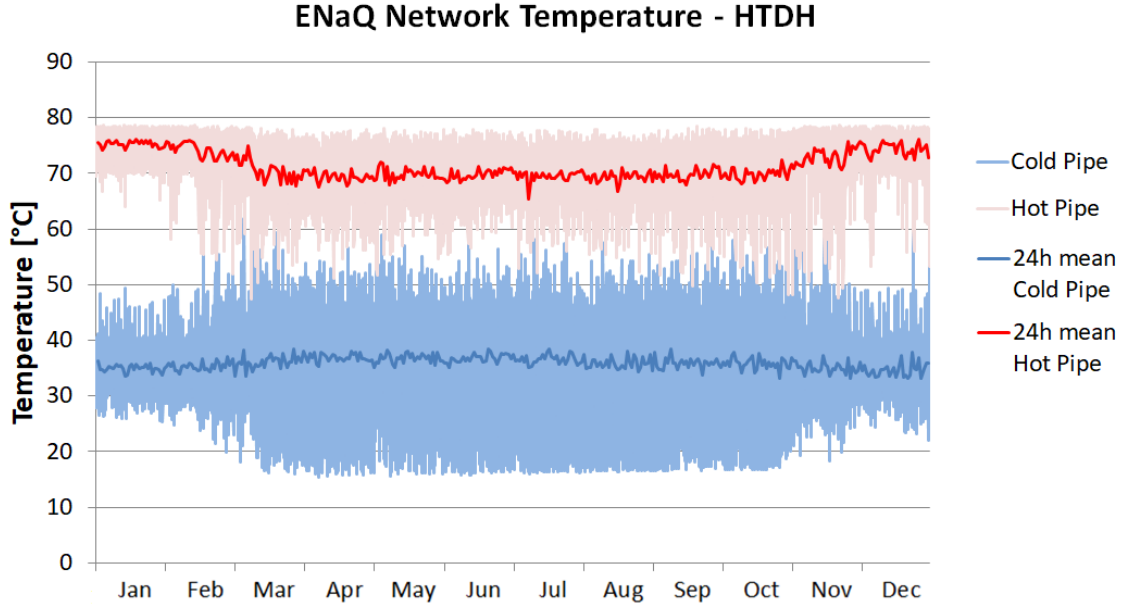


Figure 4.1: Hourly and daily network temperature at ENaQ starting scenario for one year

#### Chart remarks:

- The 24h mean supply temperature has a almost constant value of 70°C throughout the year.
- Similarly, the 24h mean return temperature has almost a constant value of 35°C.
- In summer, there is a slight drop in the supply temperature and a small rise in the return temperature.
- Also on summer, the hourly values have a wider range going from 60°C to 80°C at the supply side and from 18°C to 50°C at the return side.

The fact of having a constant 24h mean supply temperature is explained by the CHP control. The CHP turns on when the centralized storage tank temperature falls until 70°C and feeds it with water at 80°C. This 10°C gap can be observed in the hourly values too. The reason of having a constant 24h mean return temperature lies on the mass flow strategy designed for this HTDH model. The mass flow in the district network is adjusted to have a temperature difference between supply and return of  $\Delta T = 40^\circ\text{C}$ . Since the 24h mean supply temperature is constant, then the return must also be constant. In summer there is no SH demand which means that the total demand reduces. Because the energy transported in the network is less then, the  $\Delta T$  decreases. This phenomenon can be observed by the reduction of supply

and increase of the return temperature in both, hourly and 24h mean values.

Finally, also because of lack of SH demand in summer the return temperature adjusts to the domestic cold water inlet, which is 15°C for this model. That explains the hourly temperature decrease.

On the other hand, when observing Figure 4.2, the temperature behaviour in **ENaQ retrofitted scenario** network is different to the one presented before.

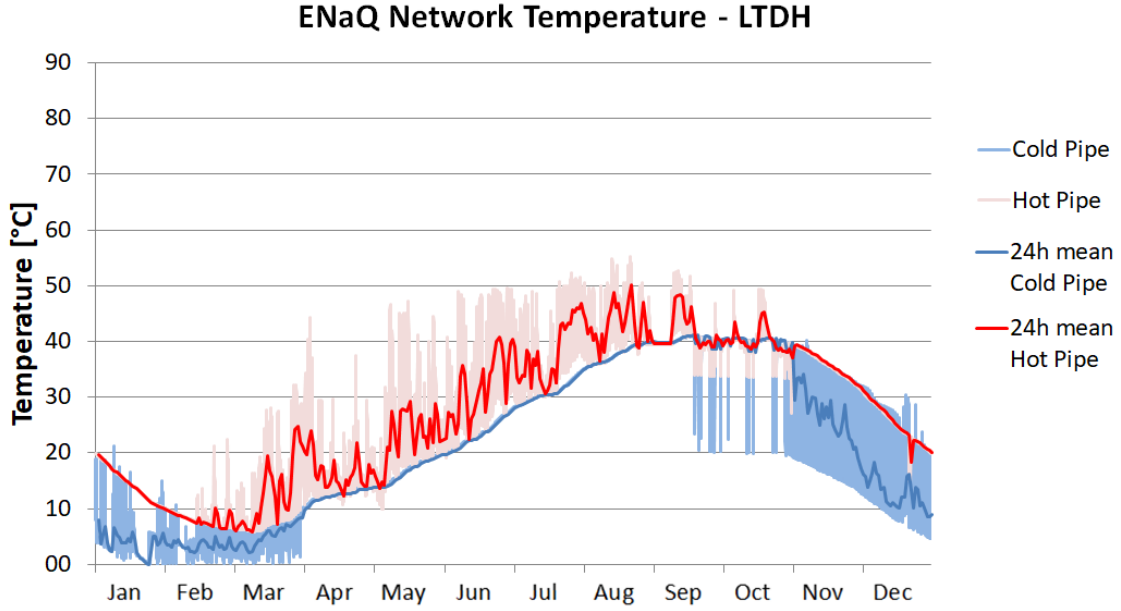


Figure 4.2: Hourly and daily network temperature at ENaQ retrofitting scenario for one year

#### Chart remarks:

- The temperature behaviour is different to the one presented before, following the LTDH reference case.
- The maximal temperature reached in this model is 48°C which happens only in some periods of August and September while the minimum temperature is 2°C at the end of January.
- The  $\Delta T$  is less than the HTDH model, with an average of 6.3°C over the year in comparison with an average of 34.6°C on the first one.

The reason that explains why these two systems have so different temperature trend lies on the different district heating system concepts of both models. In the HTDH model the network acts as a means of energy transport, from the centralized source to the decentralized sinks. This concept does not apply to the LTDH model, where the network is a connection from the decentralized sources to a centralized storage.

Because of that, in summer the temperature rises when charging the storage and in winter the temperature decreases when discharging it. This difference of systems concept can be observed in Figure 4.3: while the HTDH system transports most of the energy through the district network in winter, the LTDH system transport a part of it in winter (when discharging the seasonal storage) and the rest in summer (when charging the seasonal storage).

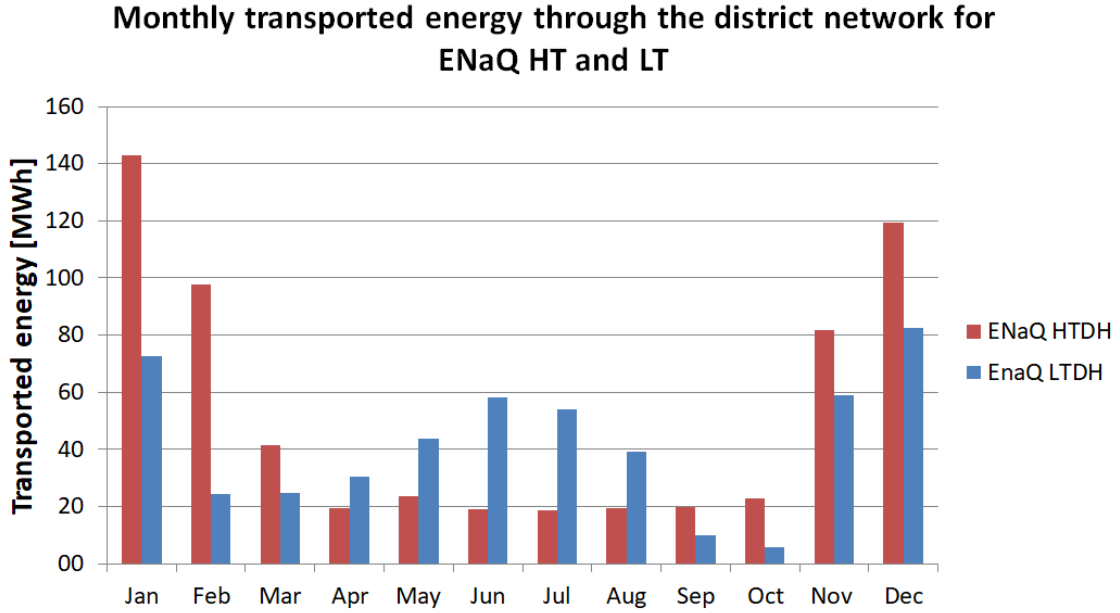


Figure 4.3: Monthly transported energy through the district network for ENaQ HT and LT

Another important point at the temperature charts is the  $\Delta T$  difference between both models. At first glance, it seems that the energy transported in the LTDH model is much less than the HTDH one, 5.5 times less to be precise. However a variable that can not be seen here is the mass flow of both models. Figure 4.4 shows the monthly transported volume through the district network for ENaQ high and low temperature district heating system. The HTDH transported volume follows the trend of the energy demand of the district while the LTDH system maintains a constant transport volume throughout the year. This constant value is possible due to the decentralized storage tanks placed on each building on the LTDH system which are able to buffer high peak demands. It is important to remark that in the LTDH the maximum water velocity restriction (see subsection 3.3) is always respected. In other words, the HTDH system has very few peaks where the maximum water velocity is reached while the LTDH constantly operates at values close to this threshold and with that, being able to transport more volume through the

network. Because of that the LTDH model is able to take from the network 41.1% of the energy that the HTDH takes even with a  $\Delta T$  5.5 times lower.

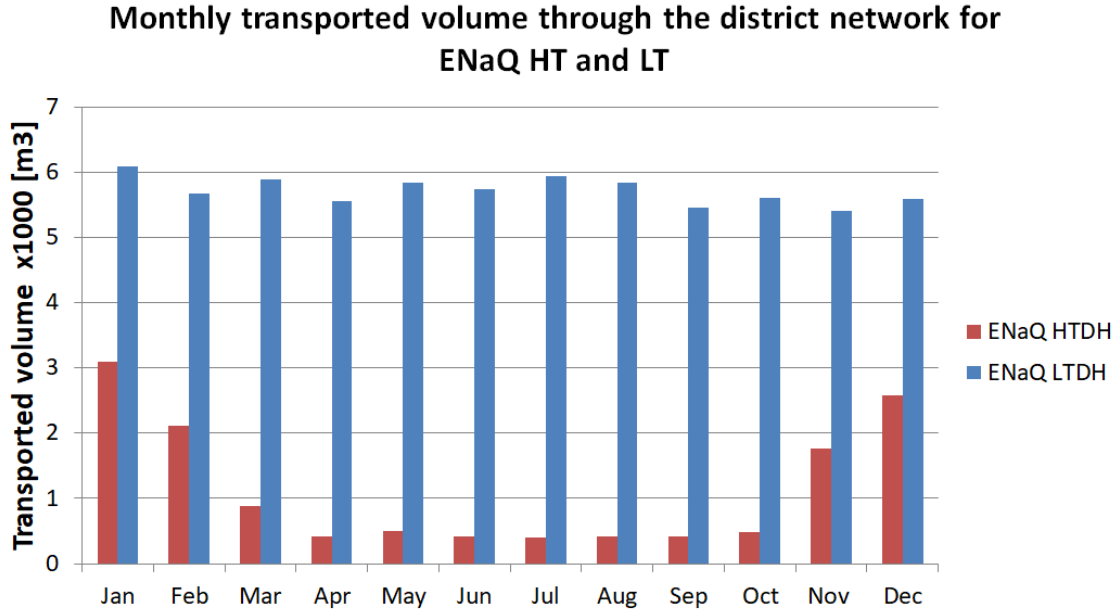


Figure 4.4: Monthly transported energy through the network for ENaQ HT and LT

Because of the possibility of reduce  $\Delta T$  and the role that the network takes in one and the other model, this transformation is not only about changing the supply system but also about changing the district heating concept which makes it possible to reduce the temperature of the system.

Going deeper in the district heating systems comparison, Table 4.1 shows the five KPI for both models.

KPI	ENaQ starting scenario (HTDH)	ENaQ retrofitted scenario (LTDH)
Share of renewable energy sources [%]	0.3	84.0
Share of electricity used in the system [%]	0.9	24.6
Energy taken from the district network [%]	98.9	41.1
Transport Losses [%]	8.3	3.4
GHG emissions [tCO <sub>2</sub> eq]	135.0	57.3

Table 4.1: KPI to compare ENaQ starting and ENaQ retrofitted scenario

**Table remarks:**

- The HTDH scenario operates almost without renewable energy sources or electricity, accounting for less than 1% each of them.
- On the other hand, the LTDH scenario operates mainly with renewable sources and almost a quarter of its energy comes from electricity.
- While almost all the energy used in the system is taken from the network in the HTDH scenario, the LTDH scenario takes less than the half of the demand from there.
- Transport losses represent a considerable number on the HTDH scenario accounting for 8.3% of the energy generated which means 52.7 *MWh*.
- The losses at the LTDH scenario reach 3.4% of the generated energy which means 20.7 *MWh*. This means that the LTDH scenario achieves a losses reduction greater than 50% compared to the HTDH scenario.
- When looking at the GHG emissions for both scenarios, there is a 57.6% reduction in LTDH scenario compared to the HTDH one.

Since the HTDH model is CHP based which works with natural gas, it is logical to observe a negligible use of renewable energy sources there. The small renewable energy share comes from the electricity use at the electric water heaters placed at the outlet of the DHW demand when there are peak loads (see subsection 3.13). Because the CHP is big enough, the use of these water heaters rarely occurs leading to a small share of electricity use in the system. Moreover, the CHP is a centralized and also the only heat generation source. Therefore practically all the energy used, is taken from the network. Due to this plus the high network temperatures presented before, and knowing that the losses are directly proportional to the temperature, the transport losses represent 8.3% of the energy generated. Finalizing with the HTDH scenario, due to the noticeable use of natural gas as energy source, greenhouse gas emissions accounts for 135 tCO<sub>2</sub>eq.

On the other hand, taking a look at the LTDH KPI, the share of renewable energy sources is high because of the CHP replacement by solar collectors, a total renewable energy source and heat pumps, a partial renewable energy source. The electrification of the supply system increases, due to the inclusion of heat pumps.

An important point to discuss is the energy taken from network, which represents 41.1% of the total energy consumed. This means that 58.9% of the demand is consumed at the same time and place where it is produced. The reason of that

is, as said before, because of the change of district heating concept from HTDH to LTDH, where decentralized sources are placed encouraging the decentralization of the system. This change of concept allows the reduction of the temperature of the system which reduces the transport losses. Here it is important to mention that this transport losses reduction occurs mainly but not only because a reduction of the network temperature. The second reason for achieving this reduction is because in the LTDH scenario, the energy transported in the network accounts for 504.2 *MWh* (238.7 *MWh* from the seasonal storage to the buildings and 265.5 *MWh* from the buildings to the seasonal storage) while this value is 626.2 *MWh* in the HTDH (all from CHP to buildings). Because of that, the energy required in the LTDH scenario is less and consequently, the temperature difference.

Finally, when looking at the GHG emissions, a reduction of 57.6% is achieved because despite the fact that the share of renewable energy sources increases from 0.3% to 84%, the electrification of the system increases too, which has a higher emission rate than the natural gas which compensate the emission level.

**After having analyzed in detail both ENaQ starting and retrofitted scenario it is possible to say that the improvement of the retrofitted scenario is considerable. An increase of RE share from 0.3% to 84.0% of the covered demand, reduction of losses from 8.3% to 3.4% of the generated energy or reduction of GHG emissions of 57.6% support the previous statement and under these KPI makes this district transformation worthwhile.**

Now the last point to address is to see under this transformation how close to **ENaQ aiming scenario** is this **ENaQ retrofitted** placed.

Table 4.2 shows the KPI values for **ENaQ retrofitted scenario** and the LTDH reference scenario. Here is necessary to mention, that from all five KPI, neither transport losses can be compared, since the network topology between ENaQ and the reference case is different, nor the GHG emissions, since the demands are different. Nevertheless these two KPI were normalized with the equivalent length  $L_{eq}$  in the losses indicator and with the demand covered in the emissions indicator in order to have a value to compare.



KPI	ENaQ retrofitted scenario	LTDH reference Scenario
Share of renewable energy sources [%]	84.0	83.0
Share of electricity used in the system [%]	24.6	26.1
Energy taken from the district network [%]	41.1	35.6
Transport Losses [ $MWh/m L_{eq}$ ]	0.6	0.8
GHG emissions [kg CO <sub>2</sub> eq/MWh demand]	98.8	104.6

Table 4.2: KPI modified to compare ENaQ retrofitted and LTDH reference scenario

**Table remarks:**

- For the first three indicators (the ones which are represented by % of the demand covered), the absolute difference in the share they provide for their scenarios is 3.1% on average.
- For both indicators, transport losses and GHG emissions there is a slight increase on the LTDH reference scenario. This increase accounts for 0.2  $MWh/m L_{eq}$  in the losses and 5.8 kg CO<sub>2</sub>eq per  $MWh$  in the emissions.

After looking at the remarks it is possible to say that even with an existent HTDH network which has the water velocity restriction (see subsection 3.3), it is possible to perform a district heating system transformation that reaches the LTDH reference scenario as if it would not have the water velocity restriction. The reason why the performance of ENaQ retrofitted scenario is slightly better, lies in the weather data from both models. EnaQ retrofitted uses Oldenburg data from year 2018 while LTDH reference scenario uses Stötten data from years 1988 until 2007. This difference in years leads to higher direct radiation in Oldenburg, which is used to increase the share of renewable energy sources as well as energy taken from network and decrease the electrification, transport losses and GHG emissions.

**Knowing that LTDH reference scenario in this case corresponds to ENaQ aiming scenario, the above means that the question established in the introduction of this master thesis has an answer: the ENaQ starting scenario can be retrofitted until ENaQ retrofitted scenario becomes ENaQ**

aiming scenario.

There are two key points that allow this transformation to happen. First, and as mentioned in Chapter 2, one of the mayor constrains when trying to reduce the district heating system temperature is that, due to the increase of mass flow required, it leads to an increase of the water velocity in the network. After performing this study, a solution to avoid this problem, is having decentralized heat sources in the LTDH model reduces the energy required from the network. This allows to comply with the water velocity constrain even when the  $\Delta T$  is reduces.

Also mentioned as a constrain in Chapter 2, is that the only way to reduce the network temperature is by reducing its return temperature. The solution of this problem is found in the second key point: each building must have a heat pump placed right before the outlet to the network connection. Thus the return temperature of the network can be lowered even to lower levels than the domestic cold water, which maximizes the  $\Delta T$  in the LTDH scenario.

## 4.2 Sensitivity analysis of ENaQ retrofitted (LTDH) scenario

As mentioned in Chapter 3 it is possibly that due to either economic or space constrains, the district heating system transformation may not be possible in its entirety. In order to see of how the system would behave if a partial transformation occurs, a sensitivity analysis was carried out. From one side, different values for solar collector field and seasonal storage tank are simulated, and for the other side the buffer storage was taken out.

### 4.2.1 ENaQ retrofitted with different solar collector area and different seasonal storage volume

Starting with the solar collector field and seasonal storage tank variation, in this subsection the KPI are presented for each size combination taking as reference the **ENaQ retrofitted scenario**. Therefore a value of seasonal storage tank of 0.8 means a tank with 80% of the reference case capacity which is  $4958 \text{ m}^3$ . The same principle is applied to the total collector field size (which is the sum of all the collectors on each building) where a size of 0.8 means a total area of  $732 \text{ m}^2$ .

Figure 4.5 shows the share of renewable energy used in the system.

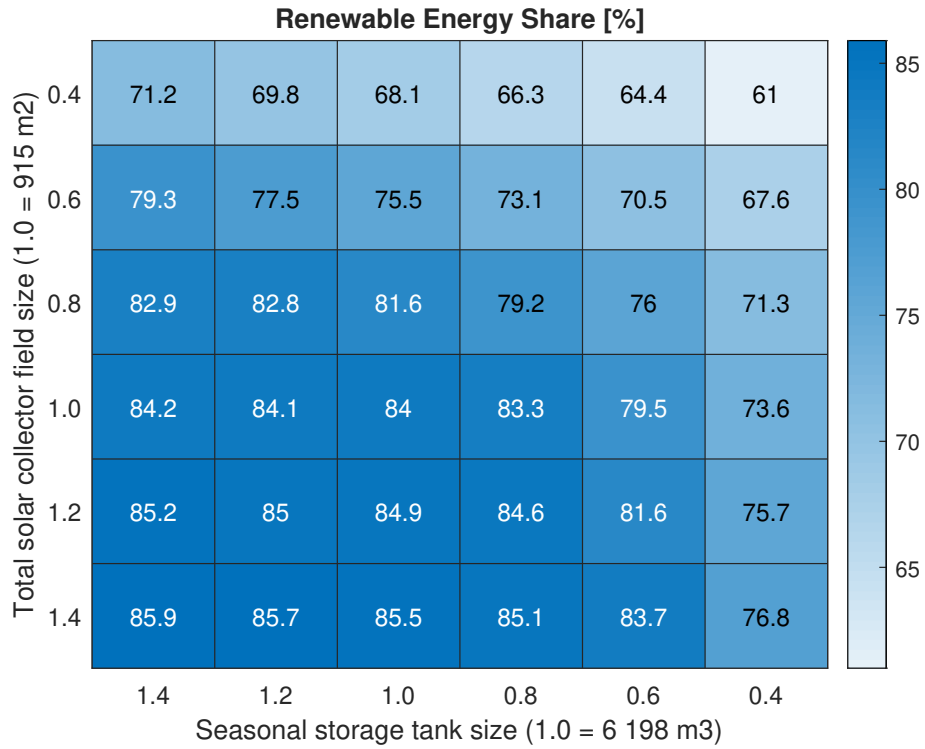


Figure 4.5: Share of renewable energy used for different sizes of solar collector field and seasonal storage tank

#### Chart remarks:

- As the size of the solar collector field grows, the RE share increases.
- Similarly, as the size of the seasonal storage grows, the RE share increases.
- The bigger the solar collector field is, the less influence in the RE share has the variation of the seasonal storage size: when the collector field size is 1.4, a variation of the seasonal storage from 1.4 to 0.4 reduces the RE share by 9.1%, but when the collector field size is 0.4, the same seasonal storage variation reduces the RE share by 10.2%.
- Doing the same procedure but now fixing the seasonal storage size, the behaviour is the same but the influence in the RE share is bigger: when the seasonal storage tank is 1.4, a variation of the collector field from 1.4 to 0.4 reduces the RE share by 14.7%, while when the seasonal tank is 0.4, the same collector field variation reduces the RE share by 15.8%.
- Finally, if both variables grow 40% of the reference case (1.4 for both), the RE share increases 1.9%. On the other hand, if both variables shrink 40% of the reference case (0.6 for both), the RE share decreases 13.5%.

Because the solar collector technology is a renewable energy source, the higher is the area of it, then the higher will the RE share be. Concerning the seasonal storage, a bigger volume of it leads to an increase of the heat capacity, which reduces the temperature rise for the same amount of stored energy. With lower temperatures, the transport losses are reduced. This losses reduction is energy that now is used in the system and **is energy coming 100% from the solar collector field** (because the seasonal storage tank is used to store the surplus of energy coming from the collectors in summer and using it in winter) and therefore renewable. Because of that, higher sizes of the seasonal storage tank leads to higher shares of RE.

Remarks three and four means two things. In the first place they mean that under the same ratio, a variation of the solar collector field has a higher influence in the RE share than a variation of the seasonal storage tank. This difference is explained in the way that these both parameters contribute to increasing the RE share mentioned in the previous paragraph. The collector field contributes to increase the RE share more directly (but not 100%) by increasing the area to capture solar energy. The seasonal storage tank contributes to increase the RE share indirectly when decreasing losses by having lower temperatures. Because of this, when deciding between shrinking either the solar collector field or the seasonal storage tank, by the same proportion, it is better to reduce this last one. Moreover if the seasonal storage size is 0.8 of the reference case but the solar collector size increases to 1.2, then the RE share is 84,6%, which is higher than the reference case. This is not possible when the solar collector size is 0.8. Secondly, remarks three and four mean that a variation of any of these two variables is not lineal: when the size of the variables are smaller than the reference case, a variation of them has a higher impact on the RE share than when they are bigger than the reference case. For the solar collector field it is explained by the minimum energy required to turn on the match flow pump: with smaller areas of collector, this threshold is more difficult to reach in order to turn on the collector pump. Due to this, on some days where in the base case the collector pump is on, in these scenarios it is off. For the seasonal storage it has to do with the temperature difference between the soil and the district network: with smaller seasonal storage tank sizes, the district network temperature increases more, making the losses higher. When the seasonal storage tank is big enough (e.g. reference case) the temperature difference between the district network and the soil becomes increasingly irrelevant to the point where the temperature difference can no longer be reduced

Finally, the reduction of the RE share is seven times more than the increase when

they shrink by 40% than when they growth by the same proportion. This, and the small variations in the RE share in the nearby of the reference case shows that in the surrounding area the change of RE share is not that big (1.5% on average with all the adjacent points) and may even be withing the error range of the model, which also means that the general sizing rules are meaningful. Besides that, it also shows that an optimization of the system components was not part of this work and could be a future work.

Figure 4.6 shows the share of electricity used in the system.

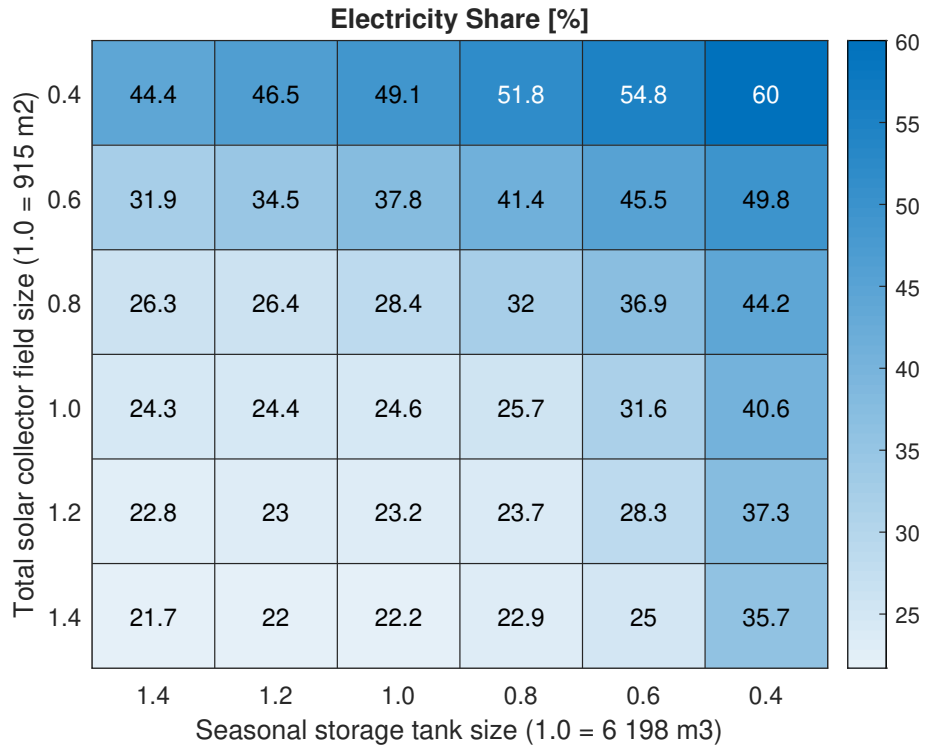


Figure 4.6: Share of electricity used for different sizes of solar collector field and seasonal storage tank

#### Chart remarks:

- The trend observed here is the same as Figure 4.5 presents.
- However the proportionality is the other way round, bigger sizes of the variables leads to less electricity used and vice versa.
- The variation range is higher, with variations of 38.5% in the extreme points while in RE shares was 24.9%.

Because the non-renewable energy used in this system, only comes from the electricity, both RE and electricity share, have the same trend. For that reason, the statements mentioned before are also applicable in this indicator. Nevertheless, since

the non-renewable energy represents 65% of the electricity used, then the variation range shrinks in the RE share. In other words, when the electricity share covers 100% of the energy used in the system, the RE share represents 35%, making the electricity share variation gap wider.

Bigger sizes of solar collector field or seasonal storage tank, allow to increase the use of solar energy, and therefore reduces the energy that needs to be covered by electricity. However, the electricity share indicator can never be equal to zero since a key component of the system, the heat pumps, make use of electricity. The previous means that the electricity used on the system can be divided into two components: the one which goes to the heat pumps, and the one which goes to the electric water heaters. The first component can not be removed while the second one can be, if the variables size are big enough.

Figure 4.7 shows the share of energy taken from the network. Here it is important to remark the difference between the transport and taken energy. The transport energy is the energy that goes and comes to/from the seasonal storage, while the taken energy from network (the one covered under this indicator), is only the energy that goes from the seasonal to the buildings.

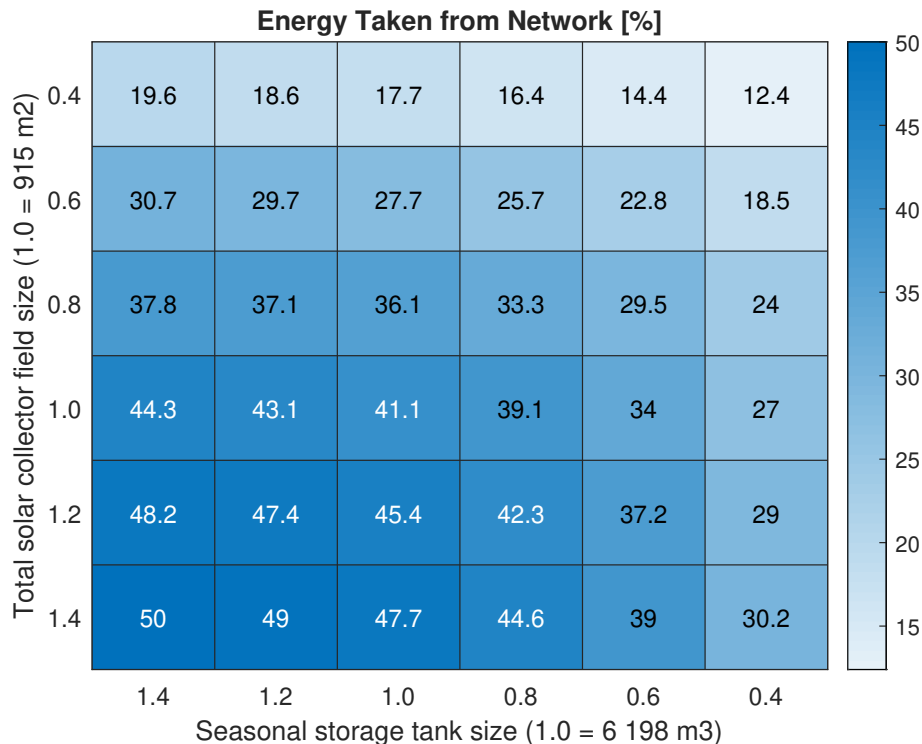


Figure 4.7: Share of energy taken from network for different sizes of solar collector field and seasonal storage tank

**Chart remarks:**

- Here the trend is also the same as the one presented in the two previous charts.
- Nevertheless the values and proportionality are different. For example, if both variables grow 20% from the reference case (1.2 for both), the energy taken from network increases 6.3%. If both shrink 20% from the reference case (0.8 for both), the energy taken from network decreases 7.8%. Doing the same procedure in the RE share, if both variables grow 20% from the reference case, the RE share increases 1.2% and if both variables shrink 20% from the reference case, the RE share decreases 5.7%.
- In other words The difference between grow or shrink both parameters 20% from the reference case is 1.5% in the energy taken form network indicator, while in the RE share indicator the difference is 4.5% which is 3 times more.
- This indicator shows that even in a scenario with plenty of space for implementing the district heating system transformation, the half of the energy is taken from the network.

To understand this indicator it is important to remember that in this model, the network is a link between the seasonal storage and the decentralized heat sources. Unlike the HTDH there is no heat source coming from the network. Because of that, the bigger are the variables size, the more energy can be stored in the seasonal storage tank and therefore, the more energy can be taken from the network.

Unlike the RE and electricity share indicators, here bigger variable sizes leads to higher increases of the indicator which means that in this case, the reference case is not close to a threshold. In other words, solar collector and seasonal storage tank sizes of 1.6 or 1.8 would lead to higher shares of energy taken from the network.

Finally, looking at the upper right values, the energy that actually is taken from the network is between 12.4% and 22.8%. This remark leads to the main question under this KPI which is to what extent is it worth having the district network if the energy taken from it represents a small portion. To answer this question, an economic analysis would need to be carried out to compare the investment costs of the district heating system transformation and the revenues obtained by the energy that comes from the network, something that is out of the scope of this master thesis.

Figure 4.8 shows the transport losses of the network, which is the energy losses over the total energy produced in the system.

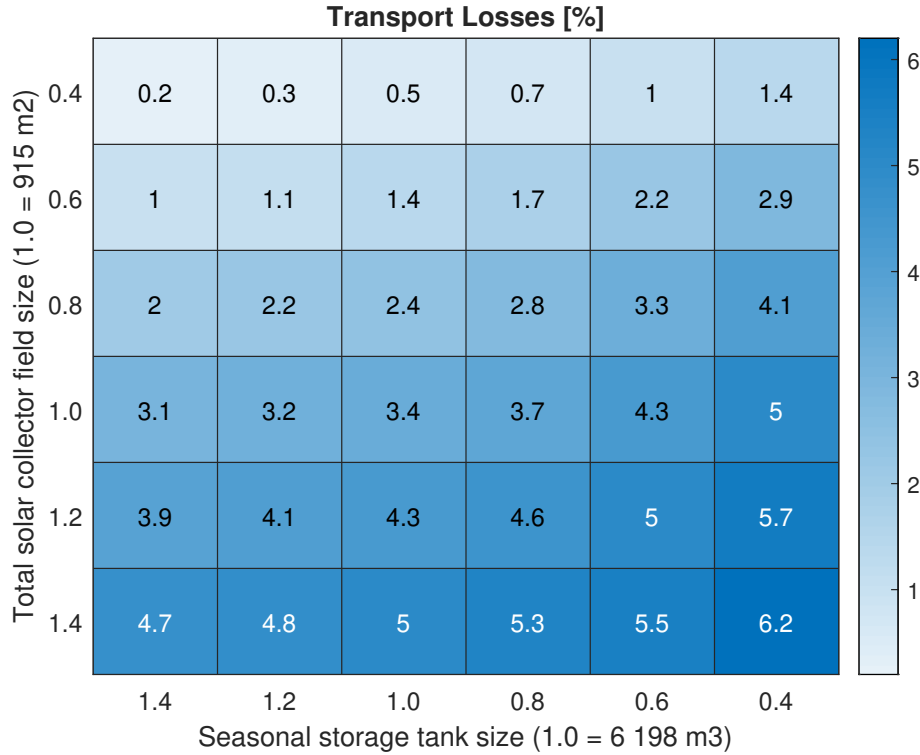


Figure 4.8: Transport losses for different sizes of solar collector field and seasonal storage tank

#### Chart remarks:

- The trend in this indicator is different from those shown before.
- Under this indicator, as the size of the solar collector field grows, the transport losses increases.
- On the contrary, as the size of the seasonal storage grows, the transport losses reduces.
- Similarly to the energy taken from network indicator, when changing the sizes of both variables by +/- 20% of the reference case, the increase or reduction of the losses changes in the same proportion: there is an increase of 20.6% of the transport losses when both variables grow 20% of the reference case (1.2 for both) and a reduction of 17.6% when both parameters shrinks by 20% of the reference case (0.8 for both).
- In all cases presented in the figure, the transport losses are less than the HTDH model.



When observing the transport losses, the smaller the solar collector field is, the less energy is delivered to the seasonal storage tank. Due to this, less energy is transported in the network and therefore less losses will have the system.

By looking at the seasonal storage size, the bigger it is, the lower the network temperature is and consequently the lower the losses are. The previous statements explains why under this indicator, the optimum is located at the top left, and not at the bottom left. Because the transport losses have a direct relation with the energy taken from network indicator, here the reference case is not close either to a threshold as the first two KPI are.

A considerable point here, is that even in the worst case, the transport losses are still smaller than the ones on the HTDH scenario, reaching 38.2 *MWh*, which is 14.5 *MWh* less then the **ENaQ starting scenario**.

Finally, figure 4.9 shows the emissions generated in one year for each scenario.

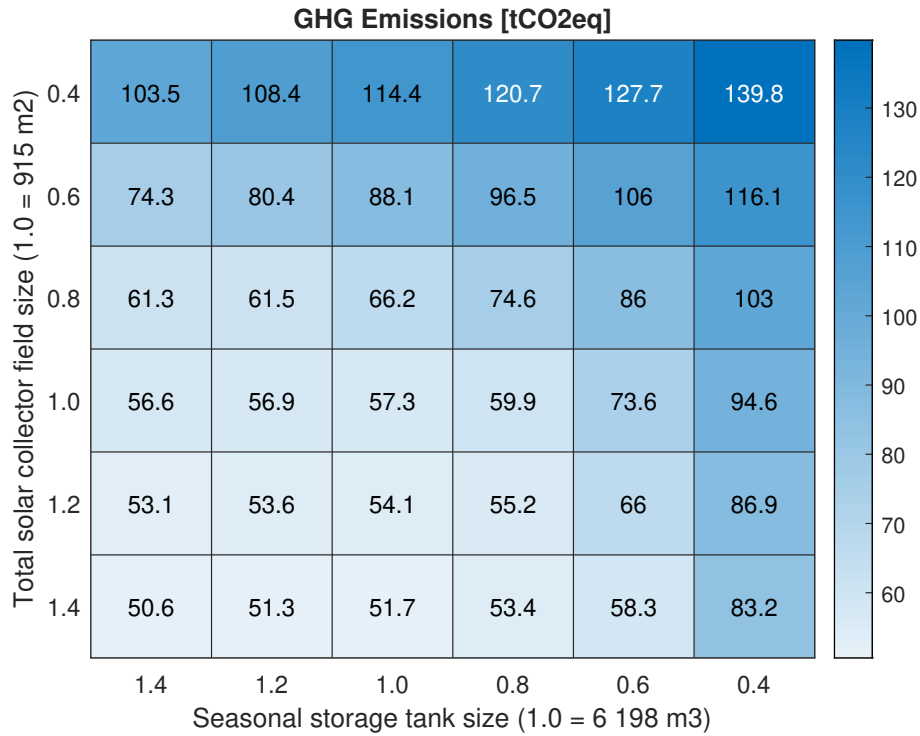


Figure 4.9: Greenhouse gas emissions for different sizes of solar collector field and seasonal storage tank

#### Chart remarks:

- The trend under this indicator is again the one shown for the first three indicators.
- Same as the RE and electricity share, an increase of both variables by 20%

of the reference case (1.2 for both) improves the indicator performance 6.5% while both variables shrinks 20% from the reference case (0.8 for both) the indicator performance decreases 30.2%

- Unlike the transported losses indicator, here when both variable's sizes shrink to 0.4, the emissions are more than the HTDH scenario, leading to a worst scenario than the current one.

The emissions on this model, come only from the electricity used in the system. Because of that, this indicator behaves the same as the electricity share indicator. The previous explains why the trend here is the same as the first two indicators. This indicator also shows, that it is definitely not worth to perform the system transformation if both the solar collector field and the seasonal storage tank have a size of 0.4, since in this case, the emissions are greater than the actual scenario. Going further with this statement, and looking at the nearby zone of the worst scenario, the GHG emissions are close to the HTDH scenario. Because of that, and same as the energy taken from network indicator, the main question of this indicator is to what extent is it worth to perform the system transformation if the emissions are reduced only a small portion. Same as before, to answer this question, an economic analysis would need to be carried out where now a carbon tax should be included in the operational costs of the analysis.

After analyzed all five KPI, it is possible to generate general guidelines for when either the seasonal storage size or the solar collector field is limited. It is important to remark that each indicator, as seen before, has its own behaviour so, for following a specific indicator, it is necessary to look only at its specific chart. The general guidelines are divided into three sections and presented below.

#### **1. Strategy when the seasonal storage space is limited:**

- If it reaches 0.8 of the reference case: there is no mayor problems. The system performance decreases 4.7% on average.
- If it reaches 0.6 of the reference case: here is a system performance decrease of 21.2% on average. To deal with this fall, an increase of the solar collector field size to at least 1.2 is suggested. This measure is not enough to bring it to the reference case, but it cushions the loss of performance, by reducing the system performance decrease to 17.9% on average. If the solar collector field increases to 1.4 the system performance decreases to 14.1%.

- If it reaches 0.4 of the reference case: here the system performance is really affected falling on average 44.8% from the reference case. Electrification, GHG emissions and transport losses are the most affected indicators falling 65.1%, 65.0% and 47.1% respectively, to the point where the question, if the transformation is worth doing, becomes relevant. Increasing the size of solar collector field slightly reduces the fall of the average performance to 42.0% and 41.5% for sizes of 1.2 and 1.4 respectively.

## 2. Strategy when the solar collector field space is limited:

- If it reaches 0.8 of the reference case: there is no mayor problem. The system performance decreases 3.3% on average. The fall on average is less than when the seasonal storage reaches 0.8 because here the transport losses indicator improves by 29.4%. Nevertheless when this indicator is excluded the system performance decreases on 11.5%.
- If it reaches 0.6 of the reference case: here the system performance is considerably affected falling on average 18.2% from the reference case (30% without transport losses indicator). Electrification, GHG emissions and energy taken from the network are the most affected indicators falling 53.7%, 53.6% and 32.6% respectively, to the point where the question, if the transformation is worth doing, becomes relevant. Increasing the size of the seasonal storage tank reduces the fall of the average performance to 9.7% (29% without transport losses indicator) and 3.9% (18.0% without transport losses indicator) for sizes of 1.2 and 1.4 respectively.
- If it reaches 0.4 of the reference case: here the system performance is really affected falling on average 38.0% (55% without transport losses indicator) from the reference case. Again Electrification, GHG emissions and energy taken from the network are the most affected indicators falling 99.6%, 99.5% and 56.9% respectively. Values like 17.7% energy taken from network and 114.4 tCO<sub>2</sub>eq emitted are in most cases, not enough to make the transformation worthwhile. Even with an increase of the seasonal storage to 1.4 of its reference case, the energy taken from network becomes 19.6% and the emissions 103.5 tCO<sub>2</sub>eq.

## 3. Strategy when both solar collector field and seasonal storage tank are limited:

- If both reach 0.8 of the reference case: here the system performance decreases 17.0% on average. Electrification and emissions indicators, the

most affected ones, fall both by 30.1%. Transport losses performance increases by 17.6%

- If both reach 0.6 of the reference case: here the system performance is really affected falling on average 46.1% from the reference case. Under this values the question, if the transformation is worth doing, becomes relevant.
- If both reach 0.4 of the reference case: the system performance falls 77% on average compared to the reference case. Performance falls like 143% in electrification or 70% in energy taken from network makes the transformation definitely not worthwhile.
- For cases when one variable is 0.8 and the other 0.6, or one is 0.8 and the other 0.4, the KPI have so different values that each case needs to be analyzed particularly. Nevertheless as general trend if the solar collector is 0.8 and the seasonal storage 0.6 there are still chances that the transformation is worth it, when the solar collector is 0.8 and the seasonal storage is 0.4 or the solar collector is 0.6 and the seasonal storage is 0.8 the system performance is really affected to the point where the question of whether the transformation is worthwhile becomes relevant. If the collector is 0.4 and the seasonal storage is 0.8 it is very likely that the transformation is not worth it.
- For cases when one variable is 0.6 and the other is 0.4, it is very likely that the system transformation is not worth due to already with the case 0.6 for both variables the system has a bad performance.

#### **4.2.2 ENaQ retrofitted with only one decentralized storage tank**

The ENaQ system with only one decentralized storage described in subsection 3.5.2 was modeled and simulated for one year. The five KPI that allow to observe the system performance were calculated and compared with the ENaQ reference case, which is the system with two decentralized storage tanks (the on-demand and buffer storage tanks) as Table 4.3 shows.

KPI	ENaQ retrofitted with two decentralized storage tanks	ENaQ retrofitted with one decentralized storage tank
Share of renewable energy sources [%]	84.0	78.5
Share of electricity used in the system [%]	24.6	33.2
Energy taken from the district network [%]	41.1	35.0
Transport Losses [%]	3.4	1.8
GHG emissions [tCO <sub>2</sub> eq]	57.3	77.5

Table 4.3: KPI comparison between ENaQ retrofitted with one and two decentralized storage tanks

**Table remarks:**

- The share of renewable energy sources used in the model with one decentralized storage tank decreases slightly from 84% to 78.5% which means that 32.1 *MWh* less of renewable energy are used in one year (488.1 *MWh* for 2 storage model and 456.0 *MWh* for the 1 storage model).
- On the other hand, the electricity used in the system increases from 24.6% to 33.2%, which in terms of energy means that 50.2 *MWh* more are used in one year
- The energy taken from the network decreases from 41.1% to 35.0%, which means that that 35.4 *MWh* less are taken from the district network in one year.
- Transport losses are cut by almost half, dropping from 3.4% to 1.8%. The previous means that losses went from being 20.7 *MWh* to 10.8 *MWh*.
- Finally, GHG emissions increases 20.1 tCO<sub>2</sub>eq in one year when the model operates with one decentralized storage tank.

From a general perspective the system performance with only one decentralized storage is moderately affected: when all five KPI are observed, taking into account the that the transport losses indicator has a performance increase of 47.1%, the one storage system losses 8.8% performance in comparison with the two storage

system. When the transport losses indicator is taken out, the system has a drop in performance of 22.8%.

The drop in share of renewable energy sources is due to the loss of energy coming from the solar collector field which is covered by electricity. This energy loss occurs when the collectors reach a temperature above 25°C and the heat pump is on. In that situation the solar collectors stop gaining energy (unlike the 2 decentralized storage model in which energy is still generated) and start to discharge the energy gained until this point to the seasonal storage through the district network which has a limited capacity to transport energy. This situation occurs on sunny winter days, something that happens not regularly, and because of that the amount of energy lost is 32.1 *MWh* in comparison with the two decentralized storage system.

The increase of electricity used in the system has two reasons. From one side, in the same situation described above, there are some days in winter where the heat pump should work but it can not do it because of a higher inlet temperature. For these situations, the electricity water heater placed inside the on-demand storage tank turns on and provides the extra energy needed at that moment. The second reason that leads to a higher share of electricity used in this system involves the heat pump. In the two storage system, the buffer storage was the inlet to the heat pump. This buffer storage was hot at the top and cold at the bottom. Moreover when there were solar gains, keeping the top of the buffer storage tank around 20°C in winter, they were retained there until the heat pump made use of them. The temperature at the top of the buffer storage only started to decrease in mid-February after the heat pump works continuously throughout January and even there, some solar gains increased the temperature for some hours. Without the buffer storage, the inlet temperature for the heat pump, which is set to be on the whole winter period, decreases because the direct connection to the seasonal storage. Moreover, when there are solar gains, they must be used in the very same time they are produced, because there are not option for storage them. This decrease in the inlet temperature of the heat pump leads to a reduction in the COP of it, and therefore leads to an increase of the electricity used to pump the same amount of heat. This increase in electricity used in this system is the reason for the GHG emissions increase. When comparing this increase with the solar collector and seasonal storage sensitivity analysis, it is comparable to the scenario when both solar collector field and seasonal storage size reduces to 80% of the reference capacity.

The reduction in the energy taken from network indicator is explained because of the reduction of solar energy gained in this system. In order to have an energy balance

equal to zero in the seasonal storage, the energy taken from there must be the same as that given. As said before the cut off in winter when the collector field reaches  $25^{\circ}\text{C}$  reduces the energy sent to the seasonal storage and therefore the energy taken from it.

Finally because of less energy transported in the district network along with the impediment to overcome temperatures higher than  $25^{\circ}\text{C}$  in most part of the year, leads to a strong losses reduction, specially in summer when the buffer storage was able to store higher temperatures that with this model is not possible.

One mayor challenge in this system that was mentioned in subsection 3.5.2 was the daily change of the flow direction in the district network during winter. Figure 4.10 shows the control signal for the flow direction in the district network for the one decentralized storage tank system. The figure shows the first week of February (winter) in an hourly time step. When the flow direction signal is 1, it means the building is taking energy from the district network (seasonal storage) and the mass flow in the district network flows in one certain direction. When the flow direction signal is 0, it means the building is giving energy to the network (seasonal storage) and the mass flow in the district network flows in the opposite direction of the previous case.

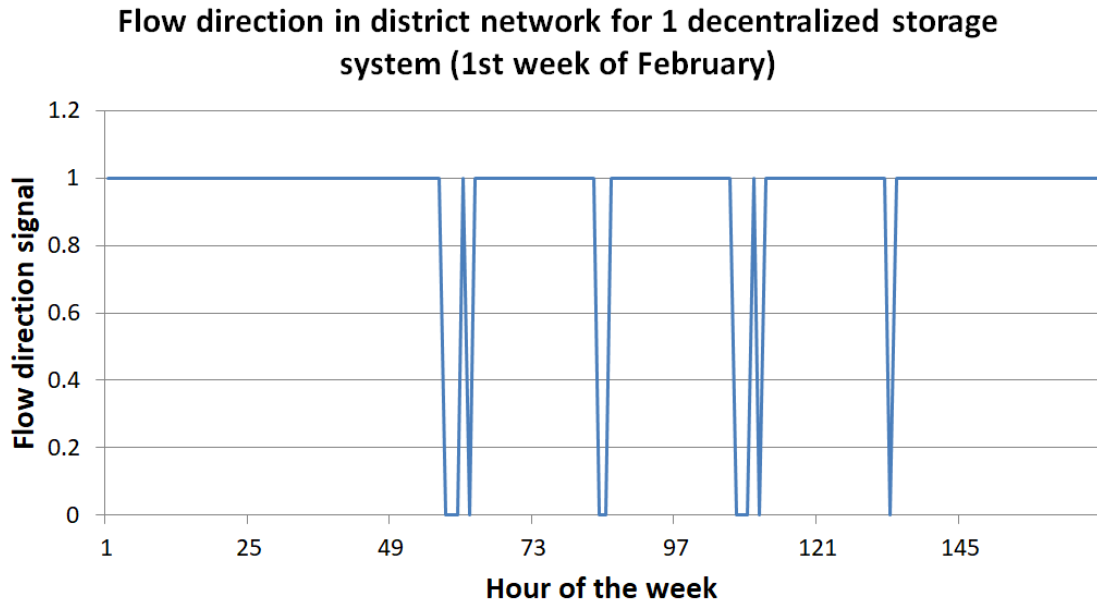


Figure 4.10: Flow direction signal in the district network for the one decentralized storage tank system

In the previous figure, there are four of seven days, where the solar collector field reaches temperatures above  $25^{\circ}\text{C}$  and therefore a charging process needs to be carried

out. This seasonal storage charging process changes the direction of the mass flow in the district network for one or two hours until the collector outlet temperature return to levels below 25°C.

On the other hand, Figure 4.11 shows the same signal in the same period of the year but for the two decentralized storage tank system.

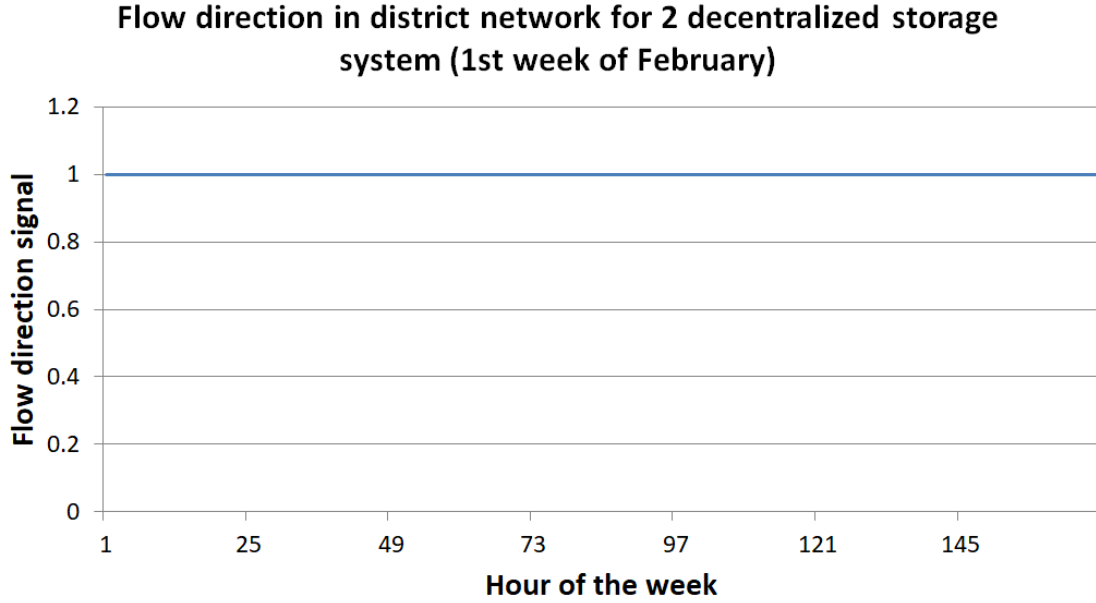


Figure 4.11: Flow direction signal in the district network for the two decentralized storage tank system

In this figure the flow direction signal has a constant value of 1, which means that the mass flow inside the district network flows always in the same direction: from the seasonal storage to the buildings.

This change of mass flow direction presented in the one storage system represents an hydraulic challenge that needs to be studied in detail and is out of the scope of this master thesis.

To finalize this section, it can be said that there is a trade off between taking out the buffer storage on each building and reducing the system performance by 8.8% on average (22.8% without the transport losses). Nevertheless, the most important issue here is to study the feasibility of changing the mass flow direction in the district network for shorter periods in winter.



# Chapter 5

## Conclusion and Future Work

### 5.1 Conclusion

After discussing the results obtained in this master thesis, there are three main conclusions that can be derived from this work.

The first main conclusion concerns the development and validation of a LTDH model in the Carnot Toolbox. This model is based on the model from the study entitled *Potenziale von Niedrigtemperaturnetzen zur Steigerung des Anteils erneuerbarer Energien in Quartieren* developed by the Technical University of Munich in 2017 [28]. The Carnot Toolbox model makes use of one building in the district and scales it up to represent the whole district heating system. Because of that, a method to represent the district network in a two single pipes was also developed and validated. The Carnot Toolbox model reliably represents the holistic behaviour of the system and the differences between the results and the TUM ones are well argued. Because of that, it is possible to say, that now there is a validated LTDH model that can be used in the future to simulate and evaluate different district heating systems.

The second conclusion of this work, and the most important one, concerns the district heating system transformation from high to low temperature (for this master thesis from 3<sup>rd</sup> to 4<sup>th</sup> generation of district heating systems). Under this point it can be said, that it is technically possible to perform the transformation to the very low temperature system. There are two key points that must be implemented to achieve this transformation. The first key point is to place a heat pump at the connection of the district network with each building. Due to the lower temperature levels usable by the heat pump, the return temperatures in the network can be strongly reduced (thereby also reducing losses). The second key point is to implement decentralized

heat sources on each building. These sources reduce the energy that must be transported in the district network and because of that, the  $\Delta T$  in the network can be reduced without increasing the mass flow inside of it. This means that the water velocity of the network does not increase even when the temperature difference between supply and return temperature reduces. Because of these two key points, it is also concluded that this district heating system transformation is not only about replacing heat sources. This transformation is a system concept transformation, where the district network is no longer a connection between source and demand, but is connection between the buildings and the seasonal storage to store the surplus of energy in summer and use it in winter.

The previous conclusion address the technology transformation. Nevertheless, sometimes in reality, despite the technology is available, space or economic constrains do not allow the district transformation to happen. This previous statement, leads to the third conclusion of this work, which are guidelines for when the transformation can not be 100% performed. These guidelines are divided into four sections, which are presented below taking into account that the nominal values are those presented in the LTDH scenario ( $0.061 \text{ } m_{coll}^2/m_{living \text{ area}}^2$  and  $10.6 \text{ } m_{ss \text{ tank}}^3/MWh_{demand}$ ):

- **Guideline for when the seasonal storage tank is limited:** if the size of it is 80% of the nominal value, the transformation is worth it presenting small declines on its performance. If the size is 60% of the nominal value, the problem can be solved by increasing the size of the solar collector field at least 20% of its nominal value. If the tank size is 40% of its nominal value or lower, it is likely that the transformation is not feasible since there is a fall of 44.8% of the system performance compared with the reference case.
- **Guideline for when the solar collector field is limited:** if the field size is 80% of the nominal value, again there are no big problems for performing the transformation. If the field size is 60% of the nominal value, the transformation may not be feasible, even when the size of the seasonal storage tank increases. If the solar collector field size is 40% of the nominal value, it is likely that the transformation is not feasible since there is a fall of 38.0% pf the system performance (55% without transport losses indicator) compared with the reference case.
- **Guideline for when both the seasonal storage tank and the solar collector field are limited:** if both sizes are 80% of their nominal values, the transformation is worth doing presenting small declines on its performance. If both values are 60% of the nominal values, the transformation may not be

feasible. If both values are 40% of their nominal values, then the transformation is definitely not worth it since the emissions are higher than the HTDH scenario.

- **Guideline for when there is no space for two storage tank on each building:** Since the on-demand storage cannot be removed, this system takes out the buffer storage. By doing that, the system performance drops to a point where the transformation is still worth executing. However it is necessary to study if the transformation is hydraulically feasible since there are constant changes in the mass flow direction inside the district network for one or two hours on several winter days.

## 5.2 Future work

This master thesis was performed in a period of six months. Because of this, it was necessary to carefully choose what part of the problem and how deep within it, was going to be analyzed to comply with the deadlines of this project. When working on this master thesis, a lot of different ideas that were out of the scope, appeared as possible directions to develop this thesis and are presented here as possible future work. They are separated into four main directions:

1. Perform an economic analysis including the capital and operational costs of performing the district heating system transformation and compare them with the revenues of the LTDH system. After doing that, perform the same sensitivity analysis presented on this thesis, but now under the economic point of view to determine the real point in terms of cost v/s benefits, where it is worth to perform the transformation.
2. Widespread this system transformation to districts where the space heating demand is higher than the one presented here. Values of  $100 \text{ kWh}/\text{m}^2\text{a}$  and  $2000 \text{ kWh}/\text{m}^2\text{a}$  are enough to cover most of residential edification in Germany [33].
3. Address the system transformation at a component level. Detailed analysis in comparison with the holistic view that this thesis provides are necessary to understand better the challenges of this system transformation. Analyze the performance of heat exchangers, water pumps with lower temperatures or the reduction of thermal stress inside the pipes are examples of what can be done.
4. Perform a detailed thermo-hydraulic study of the district network, including

the new pressure drops coming from the new mass flows. Another important point is the transformation of the original mono-directional network into a bidirectional one. This can be done by replacing the original pumps by reversible ones and modifying the direction of valves.

# Bibliography

- [1] Klima-Allianz Deutschland (2016). *Klimaschutzplan 2050 der deutschen Zivilgesellschaft*. Bundesministerium für Umwelt, Naturschutz und nukleare Sicherheit.
- [2] United Nations (2016). *Paris Agreement*. Treaty Collection.
- [3] Bundesverband der Energie- und Wasserwirtschaft e.V. (2019). *Entwicklung des Wärmeverbrauchs in Deutschland*. Foliensatz zur BDEW-Publikation.
- [4] D. Schmidt; C. Sager; A. Kallert (2014). *LowEx communities - Optimised performance of energy supply systems with exergy principles (Annex 64)*. International Energy Agency - EBC.
- [5] H. Hecking; O. Hannes; C. Elberg et al. (2017). *Szenarien für eine marktwirtschaftliche Klima- und Ressourcenschutzpolitik 2050 im Gebäudesektor*. Deutsche Energie Agentur and Energy Research & Scenarios.
- [6] B. Oschatz; B. Mailach (2010). *Planung neuer Wohngebäude nach Energieeinsparverordnung 2009 und Erneuerbare-Energien-Wärmegesetz*. Bundesministerium für Verkehr, Bau und Stadtentwicklung.
- [7] Umweltbundesamt (2020). *Erneuerbare Energie in Zahlen*. URL: <https://www.umweltbundesamt.de/themen/klima-energie/erneuerbare-energien/erneuerbare-energien-in-zahlen#uberblick>. Accessed: 29.07.2020.
- [8] M. Deutsch; N. Gerhardt; P. Schumacher et al. (2017). *Heat transition 2030 - key technologies for reaching the intermediate and long-term climate targets in the building sector*. Agora Energiewende.
- [9] Euroheat & Power (2019). *District energy in Germany*. URL: <https://www.euroheat.org/knowledge-hub/district-energy-germany/>. Accessed: 17.07.2020.
- [10] S. Schweikardt; M. Didycz; F. Engelsing et al. (2012). *Sektoruntersuchung Fernwärme*. Bundeskartellamt.
- [11] F. Kunz; M. Kendziorzski; W. P. Schill et al. (2017). *Electricity, heat, and gas sector data for modeling the German system*. Deutsches Institut für Wirtschaftsforschung.

- [12] T. Nussbaumer; S. Thalmann (2014). *Sensitivity of system design on heat distribution cost in district heating (Task 32)*. International Energy Agency - Bioenergy.
- [13] M. Deutsch; A. Langenheld (2019). *Wie werden Wärmenetze grün?* Agora Energiewende.
- [14] Bundesgesetzblatt (2007). *Energieeinsparverordnung*. URL: [https://www.gesetze-im-internet.de/enev\\_2007/index.html](https://www.gesetze-im-internet.de/enev_2007/index.html). Accessed: 17.07.2020.
- [15] ENaQ Project (2020). *Das smart city living lab Oldenburg*. URL: <https://www.enaq-fliegerhorst.de/teilprojekte/>. Accessed: 17.07.2020.
- [16] H. Lund; S. Werner; R. Wiltshire et al. (2014). *4th Generation District Heating (4GDH): Integrating smart thermal grids into future sustainable energy systems*. Energy, 68, 1-11.
- [17] D. Schmidt; A. Kallert (2017). *Low temperature district heating for future energy systems (Annex TS1)*. International Energy Agency - DHC.
- [18] University College London (2017). *Design requirements for connections to the UCL district heating network*.
- [19] P. Woods (2015). *Heat networks: code of practice for the UK - Raising standards for heat supply*. Chartered Institute of Building Services Engineers.
- [20] G. K. Schuchardt (2016). *Integration of decentralized thermal storages within district heating (DH) networks*. Environmental and Climate Technologies, 18.1, 5-16.
- [21] Y. Xing; A. Bagdanavicius; S. Lannon et al. (2012). *Low temperature district heating network planning with the focus on distribution energy losses*. Applied Energy.
- [22] M. Köfinger; D. Basciotti; R. R. Schmidt (2017). *Reduction of return temperatures in urban district heating systems by the implementation of energy-cascades*. Energy Procedia, 116, 438-451.
- [23] H. Gadd; S. Werner (2014). *Achieving low return temperatures from district heating substations*. Applied Energy, 136, 59-67.
- [24] J. Duffie; W. Beckman (2013). *Solar engineering of thermal processes*. John Wiley & Sons. Fourth Edition.
- [25] M. Pirouti (2013). *Modelling and analysis of a district heating network*. PhD Thesis, Cardiff University.
- [26] P. Olsen; C. Christiansen; M. Hofmeister et al. (2014). *Guidelines for low-temperature district heating*. EUDP-DEA. Denmark.

- [27] S. Lohmann (2013). *Einführung in die Software MATLAB - Simulink und die Toolboxen CARNOT und Stateflow zur Simulation von Gebäude- und Heizungstechnik*. Fachhochschule Düsseldorf.
- [28] K. M. Heissler; J. Metz; W. Lang et al. (2017). *Potenziale von Niedrigtemperaturnetzen zur Steigerung des Anteils erneuerbarer Energien in Quartieren*. Technische Universität München - Zentrum für nachhaltiges Bauen.
- [29] R. Heimrath (2004). *Simulation, Optimierung und Vergleich solarthermischer Anlagen zur Raumwärmeversorgung für Mehrfamilienhäuser*. PhD Thesis, Technische Universität Graz.
- [30] H. Ren; W. Gao; Y. Ruan (2008). *Optimal sizing for residential CHP system*. Applied Thermal Engineering, 28, 514-523.
- [31] K. Juhrich (2016). *CO<sub>2</sub>-Emissionsfaktoren für fossile Brennstoffe*. Umweltbundesamt.
- [32] S. Enkhardt (2020). *Umweltbundesamt verzeichnet weitere sinkende CO<sub>2</sub>-Emissionen bei Stromerzeugung*. PV Magazine. URL: <https://www.pv-magazine.de/2020/04/08/umweltbundesamt-verzeichnet-weitere-sinkende-co2-emissionen-bei-stromerzeugung/>. Accessed: 17.07.2020.
- [33] N. Gerhardt; I. Ganai; M. Jentsch et al. (2019). *Entwicklung der Gebäudewärme und Rückkopplung mit dem Energiesystem in 95% THG Klimazielszenarien*. Fraunhofer IEE.

# Appendix A

## Heat Pump data used in the Model

The Technical University of Munich provided the data which was used in their model. Figure A.1 shows values of heat capacity, power and COP for different entering water temperatures (EWT) and mass flows (in GPM).

Source EWT	Load EWT	Source GPM	Source WPD Ft Head	3.8 GPM							7.0 GPM							8.9 GPM						
				Source LWT	Heat Cap Mbtuh	Power kW	Heat Of Absorb	COP	Load LWT	Load WPD Ft Head	Source LWT	Heat Cap Mbtuh	Power kW	Heat Of Absorb	COP	Load LWT	Load WPD Ft Head	Source LWT	Heat Cap Mbtuh	Power kW	Heat Of Absorb	COP	Load LWT	Load WPD Ft Head
70.0	60.0	3.8	1.4	56.2	30.4	1.25	26.1	7.1	76.0	1.5	56.0	30.4	1.14	26.5	7.8	68.7	5.1	55.9	30.4	1.10	26.7	8.1	66.8	8.3
70.0	60.0	7.0	4.8	61.7	33.3	1.25	29.0	7.8	77.5	1.5	61.6	33.3	1.14	29.4	8.6	69.5	5.1	61.6	33.3	1.11	29.5	8.8	67.5	8.3
70.0	60.0	8.9	7.7	63.4	33.7	1.26	29.4	7.8	77.7	1.5	63.3	33.7	1.15	29.8	8.6	69.6	5.1	63.3	33.7	1.12	29.9	8.8	67.6	8.3
70.0	80.0	3.8	1.4	57.9	29.0	1.76	23.0	4.8	95.3	1.3	57.6	29.0	1.61	23.5	5.3	88.3	4.5	57.5	29.0	1.56	23.7	5.4	86.5	7.2
70.0	80.0	7.0	4.8	62.6	31.7	1.77	25.7	5.2	96.7	1.3	62.5	31.7	1.62	26.2	5.7	89.1	4.5	62.5	31.7	1.57	26.3	5.9	87.1	7.2
70.0	80.0	8.9	7.7	64.1	32.2	1.79	26.1	5.3	97.0	1.3	64.0	32.2	1.63	26.6	5.8	89.2	4.5	64.0	32.2	1.58	26.8	6.0	87.3	7.2
70.0	100.0	3.8	1.4	59.4	28.0	2.31	20.1	3.6	114.8	1.2	59.0	28.0	2.11	20.8	3.9	108.1	3.9	58.9	28.0	2.04	21.0	4.0	106.3	6.3
70.0	100.0	7.0	4.8	63.5	30.6	2.32	22.7	3.9	116.2	1.2	63.3	30.6	2.12	23.4	4.2	108.8	3.9	63.2	30.6	2.05	23.6	4.4	106.9	6.3
70.0	100.0	8.9	7.7	64.8	31.1	2.34	23.1	3.9	116.5	1.2	64.6	31.1	2.14	23.8	4.3	108.9	3.9	64.6	31.1	2.07	24.0	4.4	107.0	6.3
70.0	120.0	3.8	1.4	60.9	27.1	2.87	17.3	2.8	134.4	1.0	60.4	27.1	2.62	18.2	3.0	127.8	3.4	60.3	27.1	2.55	18.4	3.1	126.2	5.5
70.0	120.0	7.0	4.8	64.3	29.7	2.89	19.8	3.0	135.8	1.0	64.1	29.7	2.64	20.7	3.3	128.6	3.4	64.0	29.7	2.56	21.0	3.4	126.8	5.5
70.0	120.0	8.9	7.7	65.4	30.2	2.91	20.3	3.0	136.1	1.0	65.3	30.2	2.66	21.1	3.3	128.7	3.4	65.2	30.2	2.58	21.4	3.4	126.9	5.5
80.0	60.0	3.8	1.3	65.0	32.8	1.26	28.5	7.6	77.3	1.5	64.7	32.8	1.15	28.9	8.4	69.4	5.1	64.7	32.8	1.12	29.0	8.6	67.4	8.3
80.0	60.0	7.0	4.5	70.9	35.9	1.27	31.6	8.3	79.9	1.5	70.9	35.9	1.16	31.9	9.1	70.3	5.1	70.8	35.9	1.13	32.0	9.3	68.1	8.3
80.0	60.0	8.9	7.2	72.8	36.4	1.28	32.0	8.3	79.2	1.5	72.7	36.4	1.17	32.4	9.1	70.4	5.1	72.7	36.4	1.14	32.5	9.4	68.2	8.3
80.0	80.0	3.8	1.3	66.7	31.3	1.79	25.2	5.1	96.5	1.3	66.4	31.3	1.63	25.7	5.6	89.0	4.5	66.3	31.3	1.58	25.9	5.8	87.1	7.2
80.0	80.0	7.0	4.5	71.9	34.3	1.80	28.2	5.6	98.1	1.3	71.8	34.3	1.64	28.7	6.1	89.8	4.5	71.7	34.3	1.59	28.9	6.3	87.7	7.2
80.0	80.0	8.9	7.2	73.6	34.8	1.81	28.6	5.6	98.4	1.3	73.4	34.8	1.66	29.1	6.1	90.0	4.5	73.4	34.8	1.61	29.3	6.3	87.8	7.2
80.0	100.0	3.8	1.3	68.3	30.2	2.34	22.2	3.8	116.0	1.2	67.9	30.2	2.14	22.9	4.1	108.7	3.9	67.8	30.2	2.07	23.1	4.3	106.8	6.3
80.0	100.0	7.0	4.5	72.8	33.1	2.35	25.1	4.1	117.5	1.2	72.6	33.1	2.15	25.8	4.5	109.5	3.9	72.5	33.1	2.08	26.0	4.7	107.5	6.3
80.0	100.0	8.9	7.2	74.3	33.5	2.37	25.4	4.1	117.7	1.2	74.1	33.5	2.17	26.1	4.5	109.6	3.9	74.1	33.5	2.10	26.3	4.7	107.6	6.3
80.0	120.0	3.8	1.3	69.8	29.3	2.91	19.4	3.0	135.6	1.0	69.3	29.3	2.66	20.2	3.2	128.5	3.4	69.2	29.3	2.58	20.5	3.3	126.7	5.5
80.0	120.0	7.0	4.5	73.7	32.1	2.93	22.1	3.2	137.1	1.0	73.4	32.1	2.67	23.0	3.5	129.3	3.4	73.4	32.1	2.60	23.2	3.6	127.3	5.5
80.0	120.0	8.9	7.2	75.0	32.5	2.96	22.4	3.2	137.3	1.0	74.7	32.5	2.70	23.3	3.5	129.4	3.4	74.7	32.5	2.62	23.6	3.6	127.4	5.5

Figure A.1: Heat pump data used in the reference model provided by the Technical University of Munich



With this data, curves for the heat pump regarding the source side, the heating side and the electricity consumption were derived as Figure A.2 shows. The way these curves are presented is the way the Carnot Toolbox reads them.

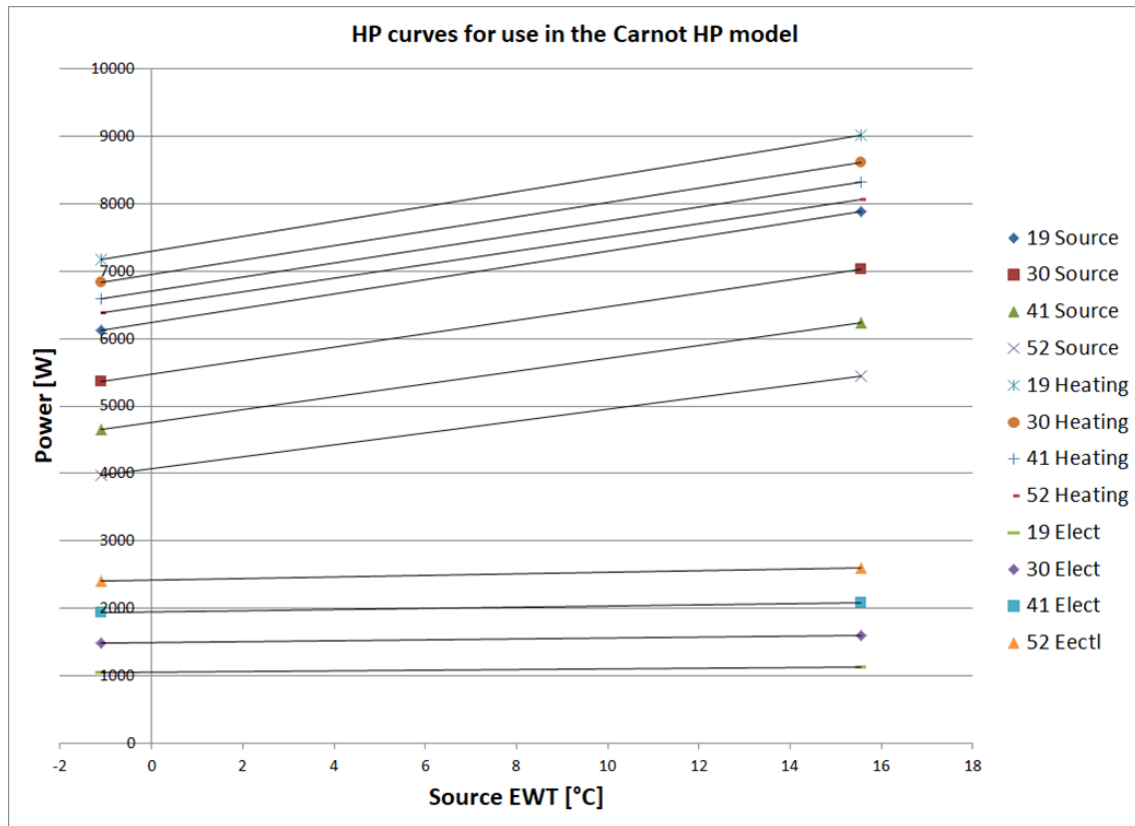


Figure A.2: Heat pump curves in the form the Carnot Toolbox uses it. Curves derived from the data provided by the TUM

# Appendix B

## Images of LTDH model developed in the Carnot Toolbox

In this section, figures of how the Carnot Toolbox model of the LTDH system in the software looks. Four different images covers all the parts of the model which turned out to be very extensive.

Starting by the solar collector field, Figure B.1 shows how the collectors components are plus the control for simulate a match flow pump.

Figure B.2 shows the on-demand storage with the demands. The electric water heater placed inside the on-demand storage is also shown. The demands are separated between SH and DHW with a flow diverter right after the water pump.

Continuing with the second storage tank in the building, Figure B.3 shows the buffer storage together with the heat pump. The load side of the heat pump has a match flow control strategy too. It is also possible to see the two heat exchangers to charge or discharge the seasonal storage.

Finally, Figure B.4 shows the district network and the seasonal storage. At the top of the figure it can be seen the scaling factors to either increase the mass flow when going to the seasonal storage or decrease the mass flow when coming back from the seasonal storage.

It is important to remark that all the figures previously shown have some simplifications in comparison with the real Carnot Toolbox model and some not important parts were taken out. This was done in order to show a clear structure of the main components of the model that otherwise would have been confuse.

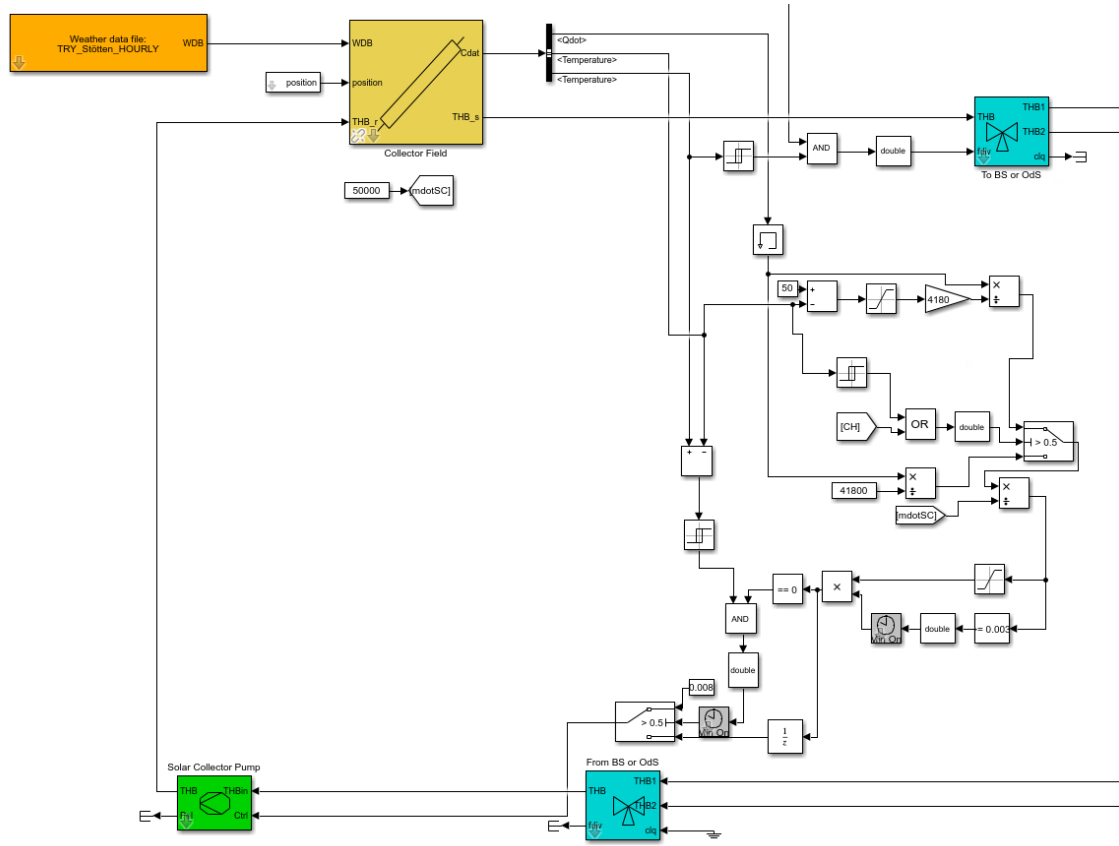


Figure B.1: Solar collector field modeled in the Carnot Toolbox

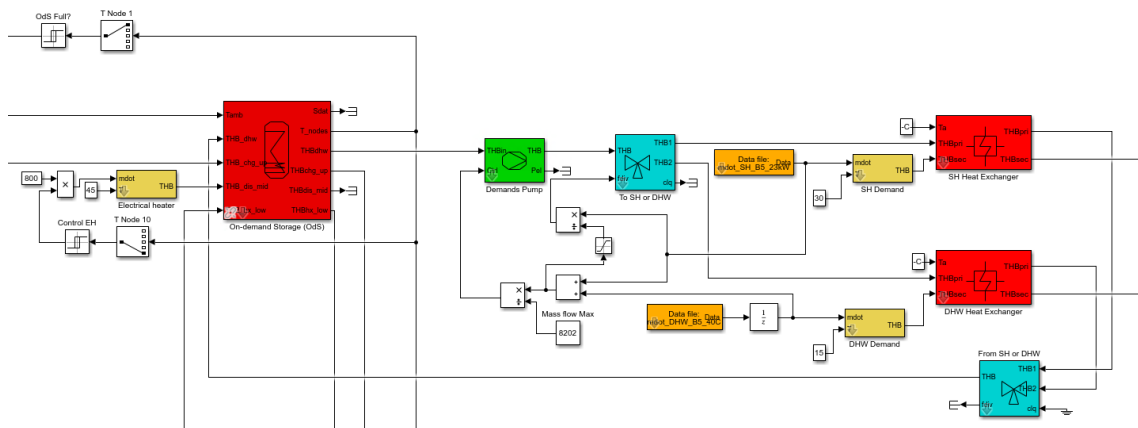


Figure B.2: On-demand storage with SH and DHW demands modeled in the Carnot Toolbox

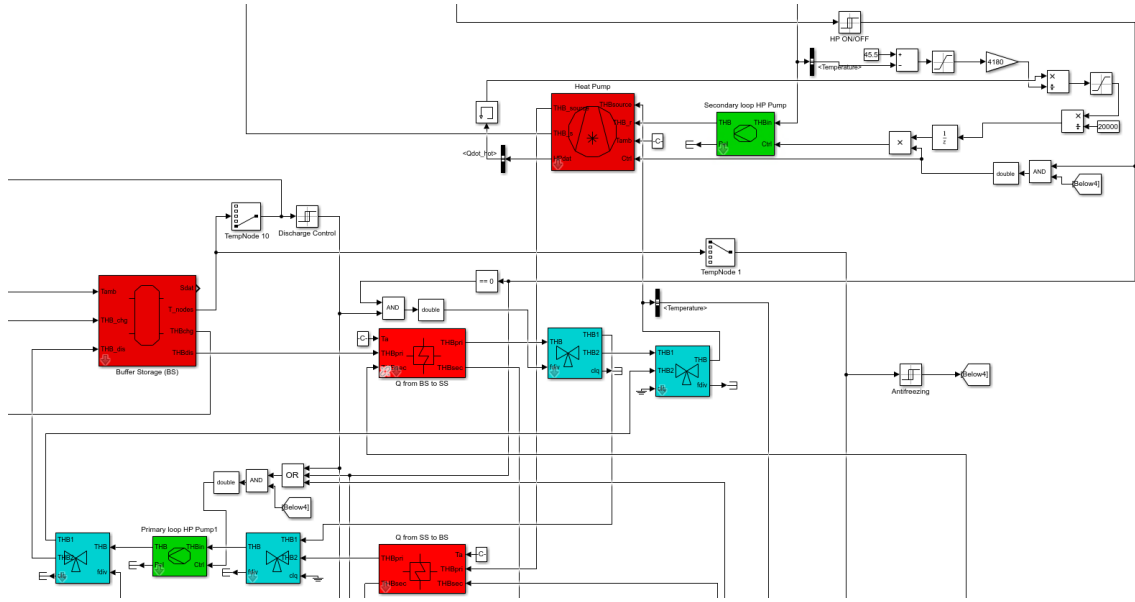


Figure B.3: Buffer storage tank, heat pump and connection with the network modeled in the Carnot Toolbox

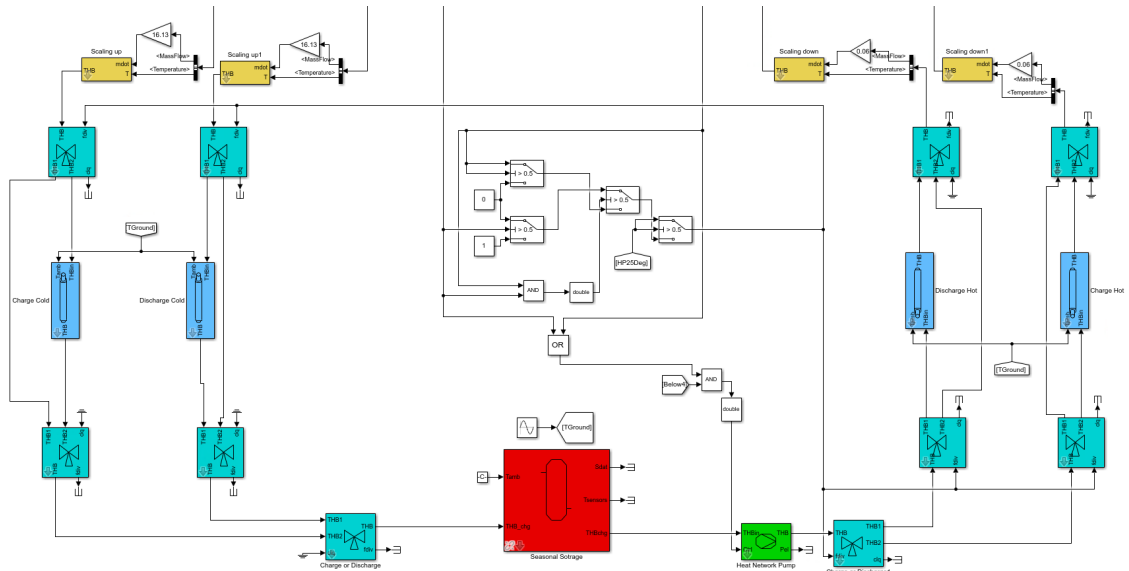


Figure B.4: District network with the seasonal storage modeled in the Carnot Toolbox